AD-A085 358   AIR FORCE AVIONICS LAB WRIGHT-PATTERSON AFB OH   F/G 9/5

MICROWAVE CHARACTERIZATION OF THE GAAS MESFET AND DEVELOPMENT O--ETC(U)

DEC 79   M C CALCATERA

UNCLASSIFIED   AFAL-TR-79-1198   NL

1 OF 1

AD A085358

END

DATE FILMED

7-80

DTIC

AFAL-TR-79-1198

MICROWAVE CHARACTERIZATION OF THE GAAS MESFET AND DEVELOPMENT OF A LOW NOISE MICROWAVE AMPLIFIER

Microwave Technology Branch
Electronic Technology Division

December 1979
TECHNICAL REPORT AFAL-TR-79-1198
Final Report: 6 April 1978 to 15 December 1979

AIR FORCE AVIONICS LABORATORY
AIR FORCE WRIGHT AERONAUTICAL LABORATORIES
AIR FORCE SYSTEMS COMMAND
WRIGHT-PATTERSON AIR FORCE BASE, OHIO 45433

NOTICE

When Government drawings, specifications, or other data are used for any purpose other than in connection with a definitely related Government procurement operation, the United States Government thereby incurs no responsibility nor any obligation whatsoever; and the fact that the government may have formulated, furnished, or in any way supplied the said drawings, specifications, or other data, is not to be regarded by implication or otherwise as in any manner licensing the holder or any other person or corporation, or conveying any rights or permission to manufacture, use, or sell any patented invention that may in any way be related thereto.

This report has been reviewed by the Information Office (OI) and is releasable to the National Technical Information Service (NTIS). At NTIS, it will be available to the general public, including foreign nations.

This technical report has been reviewed and is approved for publication.

Mark C Calcatera

MARK C. CALCATERA
Project Engineer

Alan R. Mertz

ALAN R. MERTZ, Capt, USAF
Chief, Microwave Tech & Appl Gp
Microwave Technology Branch

FOR THE COMMANDER

Donald S Rees

DONALD S. REES, Chief
Microwave Technology Branch
Electronic Technology Division
Air Force Avionics Laboratory

"If your address has changed, if you wish to be removed from our mailing list, or if the addressee is no longer employed by your organization please notify AFWAL/AADM *, W-PAFB, OH 45433 to help us maintain a current mailing list".*

SECURITY CLASSIFICATION OF THIS PAGE (When Data Entered)

REPORT DOCUMENTATION PAGE

READ INSTRUCTIONS BEFORE COMPLETING FORM

1. REPORT NUMBER: AFAL-TR-79-1198	2. GOVT ACCESSION NO.: AD-A085 358
3. RECIPIENT'S CATALOG NUMBER	
4. TITLE (and Subtitle): Microwave Characterization of the GaAs MESFET and Development of a Low Noise Microwave Amplifier	5. TYPE OF REPORT & PERIOD COVERED: Final Report. 6 Apr 78 - 15 Dec 79
	6. PERFORMING ORG. REPORT NUMBER: N/A
7. AUTHOR(s): Mark C. Calcatera	8. CONTRACT OR GRANT NUMBER(s)
9. PERFORMING ORGANIZATION NAME AND ADDRESS: Air Force Avionics Laboratory, AFAL/DHM, Wright-Patterson AFB, Ohio 45433	10. PROGRAM ELEMENT, PROJECT, TASK AREA & WORK UNIT NUMBERS: 2002/03/44
11. CONTROLLING OFFICE NAME AND ADDRESS	12. REPORT DATE: December 1979
	13. NUMBER OF PAGES: 56
14. MONITORING AGENCY NAME & ADDRESS (if different from Controlling Office)	15. SECURITY CLASS. (of this report): Unclassified
	15a. DECLASSIFICATION/DOWNGRADING SCHEDULE: N/A

16. DISTRIBUTION STATEMENT (of this Report)

Approved for public release; distribution unlimited.

17. DISTRIBUTION STATEMENT (of the abstract entered in Block 20, if different from Report)

18. SUPPLEMENTARY NOTES

19. KEY WORDS (Continue on reverse side if necessary and identify by block number)

Gallium Arsenide
Field Effect Transistor
Microwave Solid State
Low Noise Amplifier
Microwave Circuit

20. ABSTRACT (Continue on reverse side if necessary and identify by block number)

An adjustable microstrip matching technique has been developed using metallized ceramic squares (METCHIPs). A good impedance transformation over a moderate bandwidth using METCHIP matching of a low noise GaAs FET amplifier stage in the 8 to 10 GHz frequency range. An empirical model was developed for the METCHIP structure by modifying the transmission line model to account for fringing effects. An analysis of the overall circuit model showed a close correspondence with the actual measured amplifier characteristics.

DD FORM 1 JAN 73 1473 EDITION OF 1 NOV 65 IS OBSOLETE

SECURITY CLASSIFICATION OF THIS PAGE (When Data Entered)

011670

FOREWORD

This report presents matching and modeling techniques for use in the evaluation of microwave transistors. It is a final report of the AFAL in-house effort, "FET Techniques," to characterize gallium arsenide field effect transistors and to develop novel circuit applications.

This technical report was prepared by Mr. M. C. Calcatera of the Microwave Technology Branch, Electronic Technology Division, Air Force Avionics Laboratory, Wright-Patterson AFB, Ohio, under Project 2002, Task 0344. The work period for this effort extended from April 1978 to December 1979.

TABLE OF CONTENTS

LIST OF ILLUSTRATIONS

LIST OF ILLUSTRATIONS (CONT'D)

I. ADJUSTABLE MICROSTRIP MATCHING STRUCTURES

A. Introduction

A simple method of adjusting the impedance that is presented to a microwave device would be useful to obtain a low noise figure, high gain, or high output power from the device. The method(s) investigated should be simple in the sense that the circuit designer should be able to make adjustments with impedance matching elements that are easy to adjust and simple to fabricate.

The specific goal of this effort was to develop procedures that can be easily used by microwave circuit engineers to obtain a good noise figure impedance transformation for a microwave transistor amplifier stage in a microstrip circuit. The procedures developed were for gallium arsenide metal/semiconductor field effect transistors (MESFET) operating in the 8 to 12 GHz frequency range. These same procedures can also be applied to impedance matching for other microwave semiconductor devices.

B. Discussion of Candidate Approaches

There are obviously many possible distributed circuit techniques to obtain an impedance transformation in a microstrip circuit. These methods may include open or short-circuited stubs, high or low impedance line transformers, tapered lines, coupled lines, or dielectric loading. To select a candidate approach, the following criteria were used:

1. Good electrical performance
   a. low loss
   b. moderately wide bandwidth

2. Reproducible

3. Easily adjustable

4. Simple to fabricate

5. Amenable to analysis

C. Gold Ribbon Open Circuit Stub

A scheme that was initially investigated is depicted in Fig. 1. A microstrip transmission line was fabricated with a checkerboard pattern of metal squares and spaces along the center conductor strips. By connecting the center conductor to various sets of metal squares, the effective source impedance that the MESFET sees can be adjusted. This is accomplished using a metal strip of gold foil as shown in Fig. 1. The configuration can be modeled as an open-circuited stub attached to the 50 ohm microstrip line as shown by the equivalent circuit of Fig. 1. Using the well-known transmission line matching techniques for a single-stub tuner, the appropriate lengths ℓ_1 and ℓ_s can be easily found with the aid of a Smith Chart. In theory, any device impedance can be transformed to 50 ohms at a single frequency if the impedance has a positive resistance.

The stubs are fabricated by cutting an appropriate length of gold ribbon with scissors and positioning it on the circuit with tweezers. A few of these stubs were successfully thermocompression bonded by placing a piece of 25 mil alumina on the ribbon and heating the alumina with the tip of a small soldering iron for about 10 seconds.

The electrical performance of the gold ribbon stubs were very erratic. When a stub was repositioned along the length of a terminated

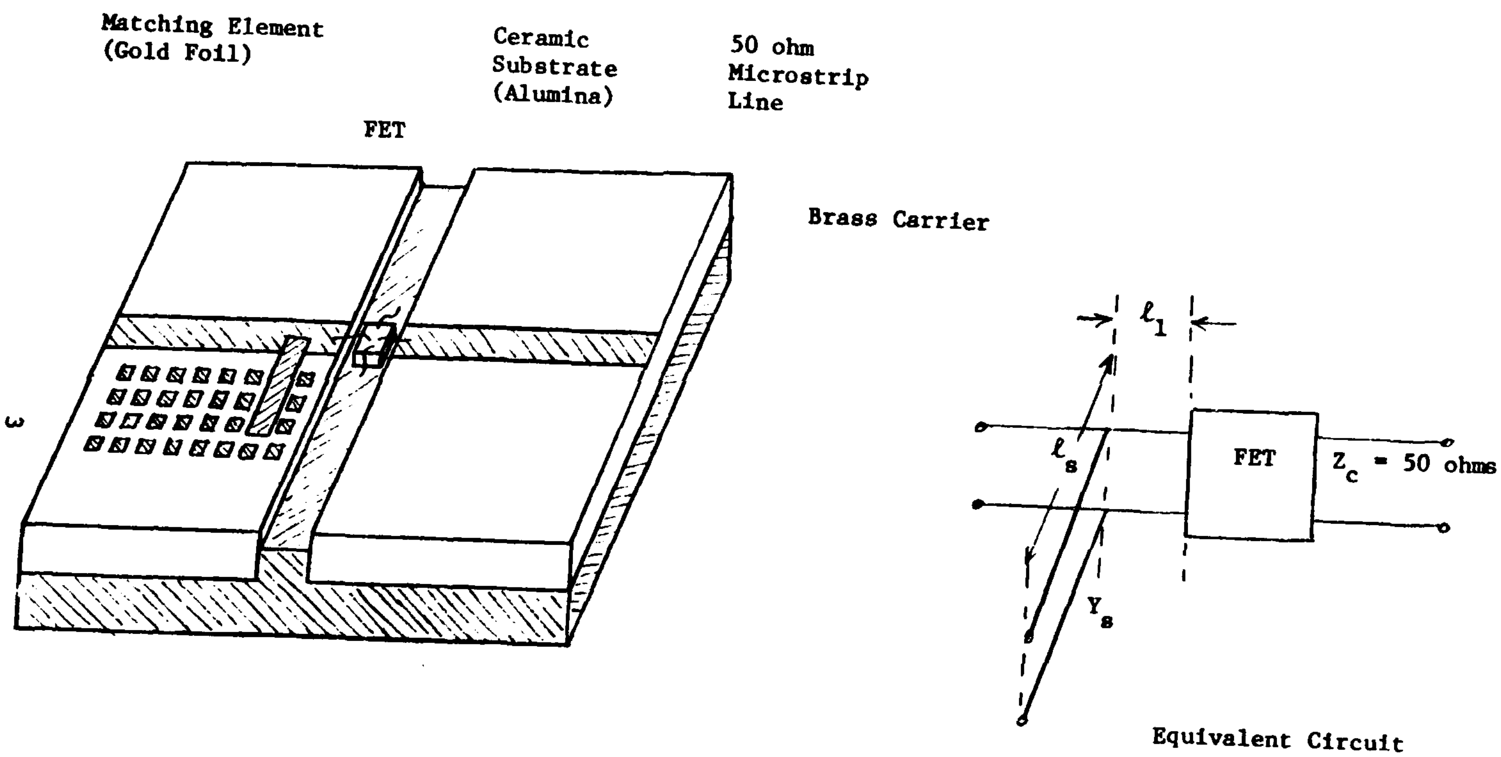

Fig. 1. Matching Circuit Using Gold Foil Open Circuit Stub

50 ohm line, the resulting reflection coefficient would typically change by up to 50%. Close inspection revealed that a small air gap of a few mils existed between portions of the ribbon and the alumina substrate. The effect of this air gap was analyzed to determine its significance. Ignoring fringing effects, the air gap reduces the effective capacitance per unit length of the stub line by:

$$\frac{C}{C_o} = \frac{1}{C_o}\left(\frac{1}{C_o} + \frac{1}{C_a}\right)^{-1}$$

$$= (C_o/C_a + 1)^{-1}$$

$$= (\varepsilon_r d_a/d_o + 1)^{-1} \qquad (1)$$

where: C_o = capacitance of line with no air gap

C_a = capacitance of the air gap

C = total capacitance (C_a and C_o in series)

ε_r = relative dielectric constant of the alumina

d_a = air gap thickness

d_o = substrate thickness

The effect is illustrated in Fig. 2. The graph shows the reduction in characteristic admittance of the stub line due to the air gap, where $Y_c/Y_{co} = (C/C_o)^{1/2}$. The shunt susceptance of the stub is given by:

$$Y_s = jB_s = jY_c \tan kL_s \qquad (2)$$

and is therefore porportional to the stub characteristic admittance Y_c. This shows that an air gap as small as 2 mils reduces the stub shunt susceptance by 25%, and explains the poor reproducibility of this matching method.

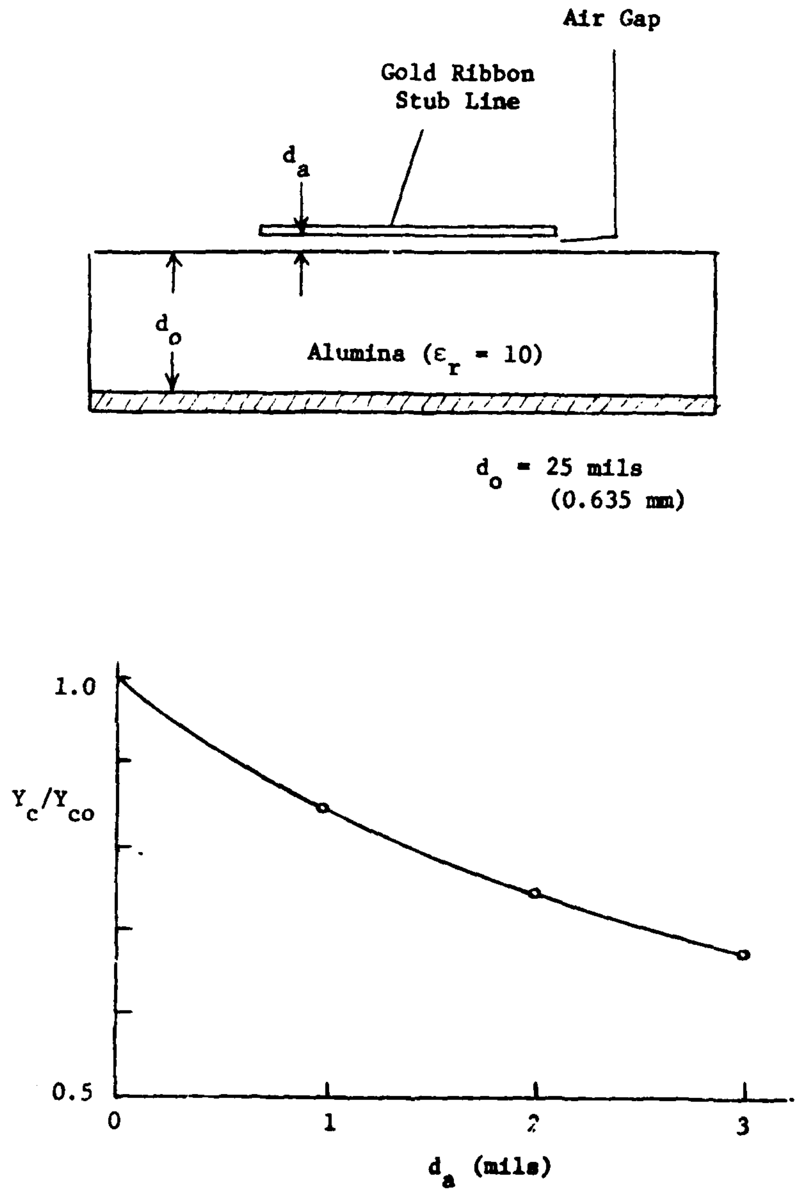

Fig. 2. Effect of Air Gap on Microstrip Line Characteristic Admittance

D. Metallized Ceramic Chip (METCHIP) Technique

Analysis of the problems with the gold ribbon tuning showed that an adjustable metallic tuning element must be capable of maintaining intimate contact with the alumina substrate in order to be reproducible. In fact a line impedance variation of under 10% requires a maximum air gap of less than 0.5 mil!

Since microwave alumina substrates are manufactured to very small flatness tolerances, a small chip cut from a metallized substrate should exhibit only a very small air gap when placed on another substrate. To test this concept, a number of small squares were fabricated using a programmable laser cutting tool. The squares ranged in size from 50 to 120 mils on a side in 10 mil increments. When centered on the microstrip conductor with the metallized side facing the microstrip center conductor as in Fig. 3, the METCHIP can be modeled as a short length of low impedance microstrip line. The line transforms a load impedance Z_ℓ to the impedance Z_ℓ' given by the familiar transmission line equation:

$$Z_\ell' = Z_c \frac{Z_\ell \cos kL + jZ_c \sin kL}{Z_c \cos kL + jZ_\ell \sin kL} \tag{3}$$

where Z_c = characteristic impedance of the line section

L = length of the line section

$k = \frac{2\pi f}{c}\sqrt{\varepsilon_r'}$ = transmission coefficient of the line section

ε_r' = effective dielectric constant of the microstrip line

Here Z and ε_r' are properties of the microstrip line that must be calculated separately. Sobol[1] gives expressions for these as follows:

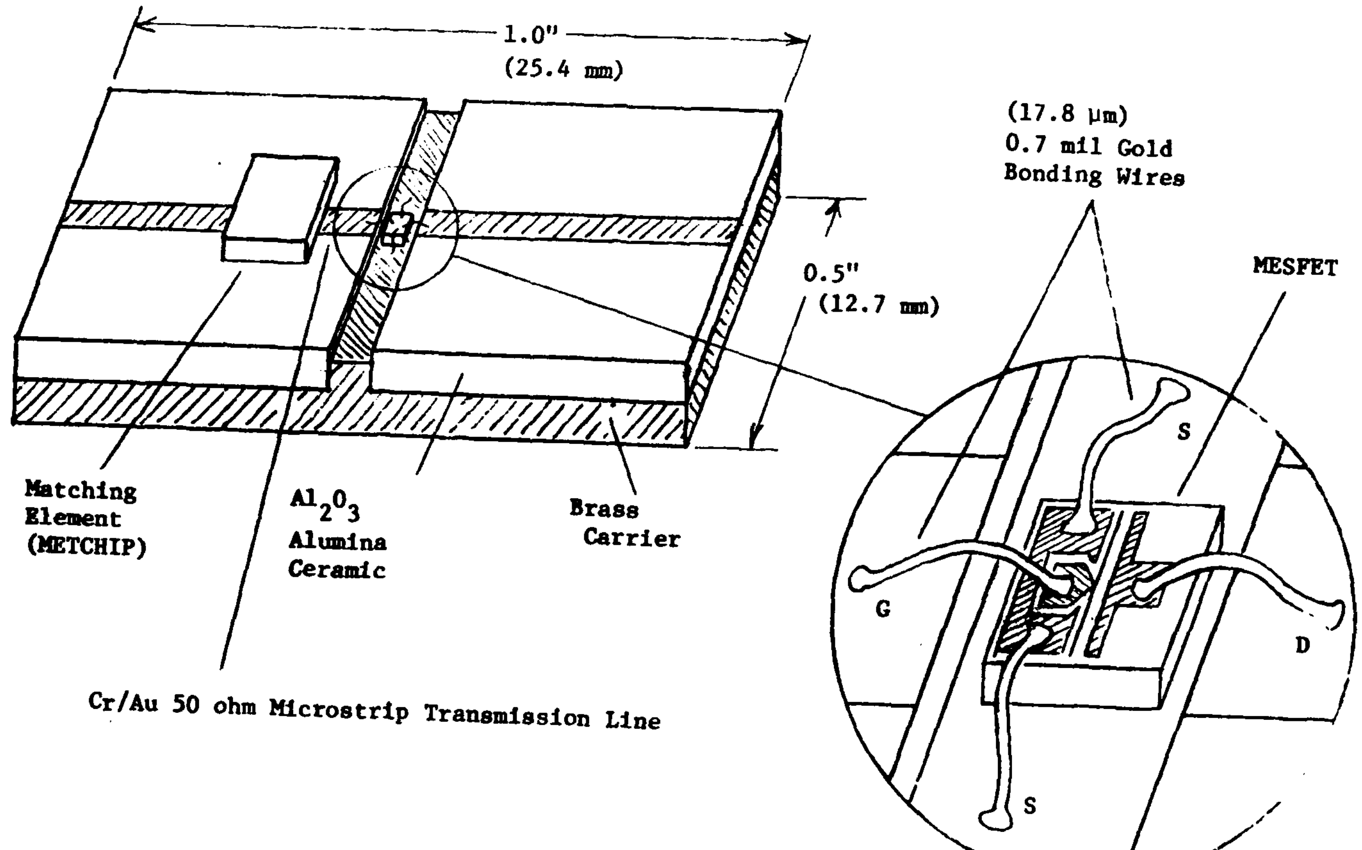

Fig. 3. MESFET Chip Carrier with METCHIP Matching Element

$$\varepsilon_r' = \varepsilon_r/(1 + 0.63\ (\varepsilon_r - 1)(W/H)^{0.1255}) \tag{4}$$

$$Z_c = \frac{376.8\ H}{\sqrt{\varepsilon_r}\ W(1 + 1.735\ \varepsilon_r^{-.0724}\ (W/H)^{-.836})} \tag{5}$$

where W = width of the microstrip line

H = thickness of the dielectric substrate

ε_r = relative dielectric constant of the substrate

These expressions were evaluated for characteristic microstrip impedances from 10 to 50 ohms, where the substrate thickness is 25 mils and the substrate material is alumina (ε_r = 10). The results are shown in Table 1. Using this data, Eqn. (3) can now be evaluated to determine the METCHIP impedances. A computer program was written in BASIC to solve Eqn. (2) for various size METCHIPs, where Z_ℓ is a 50 Ω terminated line. The resulting impedances were transformed to reflection coefficients on a 50 Ω line, where:

$$\Gamma_\ell' = \frac{50 - Z_\ell'}{50 + Z_\ell'} \tag{6}$$

The output is plotted in polar form in Fig. 4 and as functions of frequency in Figs. 5 and 6, for frequencies ranging from 2 to 12 GHz. The program listing is given in Table 2. Fig. 5 shows that METCHIPs ranging in size from 40 to 120 mils can be used to synthesize reflection coefficients in the range of 0.16 to 0.74, at any frequency in the 7 to 11 GHz range.

E. METCHIP Measurements

To check the validity of the METCHIP model as a section of low

Z0 (OHMS)	WIDTH (MILS)	DIELECTRIC (EFF)
10	247.691	8.54907
11	221.566	8.45763
12	199.786	8.3704
13	181.396	8.28718
14	165.683	8.20771
15	152.104	8.13168
16	140.261	8.05806
17	129.843	7.989
18	120.612	7.92193
19	112.379	7.85746
20	104.992	7.79544
21	98.3287	7.73573
22	92.2908	7.6782
23	86.7972	7.62277
24	81.7758	7.5693
25	77.1705	7.51769
26	72.9355	7.46791
27	69.0254	7.41982
28	65.4064	7.37338
29	62.0475	7.3285
30	58.9233	7.28514
31	56.0101	7.24324
32	53.288	7.20273
33	50.739	7.16358
34	48.3484	7.12574
35	46.1016	7.08916
36	43.987	7.05301
37	41.9934	7.01965
38	40.1114	6.98664
39	38.3321	6.95476
40	36.6476	6.92397
41	35.0508	6.89424
42	33.5357	6.86555
43	32.1262	6.85247
44	30.7798	6.8202
45	29.4985	6.78944
46	28.278	6.76009
47	27.1147	6.73203
48	26.005	6.70521
49	24.946	6.67953
50	23.9346	6.65492

Table 1. Width (W) and Effective Dielectric Constant (ϵ_r eff) of Microstrip Lines on Alumina (H = 25 mils, ϵ_r = 10) Substrates

```
DATA .76,6.99,.667,7.15,.594,7.3,.563,7.43,.488,7.55
DATA .448,7.66,.414,7.75,.386,7.84,.362,7.91
 COM A[120],C[120]
 LET M=1
 FOR L=4 TO 12
 DSPLAY "FOR W =",10*L,"MILS,Z(0),K(REL) ="
 READ G,K
 LET B1=.000532*SQR(K)
 LET B1=10*L*B1
 FOR N=0 TO 20 STEP 2
 LET B=N*B1
 LET B=TAN(B)
 CPAK(G,G*G*B,P)
  CPAK(G,B,Q)
  CDIV(P,Q,R)
  CPAK(1-REA(R),-IMG(R),P)
  CPAK(1+REA(R),IMG(R),Q)
  CDIV(P,Q,R)
  LET A[M]=MAG(R)
  LET C[M]=ANG(R)
  LET M=M+1
  NEXT N
  NEXT L
  CLEAR(1)
  LET T=0
  BUF(20)
  SCALE(2,12,0,1)
  SAXES(1,.1)
  FOR L=0 TO 88 STEP 11
  FOR M=1 TO 11
  LET N=L+M
  IF M>1 GOTO 290
  PLOT(M+1,A[N],0)
  GOTO 295
  PLOT(M+1,A[N],3)
  NEXT M
  NEXT L
  STOP
  FOR M=1 TO 11 STEP 2
  FOR L=0 TO 88 STEP 11
  LET N=M+L
  IF L>0 GOTO 350
  PLOT(A[N],C[N],0)
  GOTO 355
  PLOT(A[N],C[N],2)
  NEXT L
  NEXT M
```

Table 2. Program to Calculate METCHIP Reflection Coefficient (H-P BASIC)

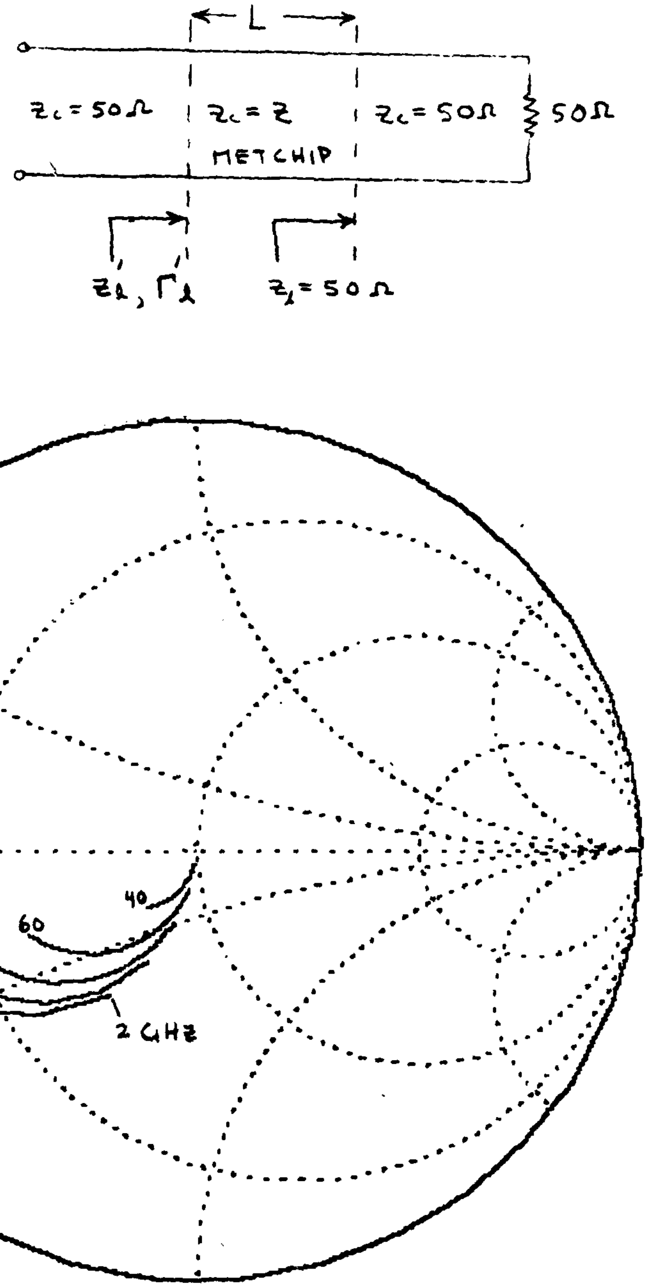

Fig. 4. Equivalent Circuit and Transformed Impedance Z'_ℓ of METCHIPs

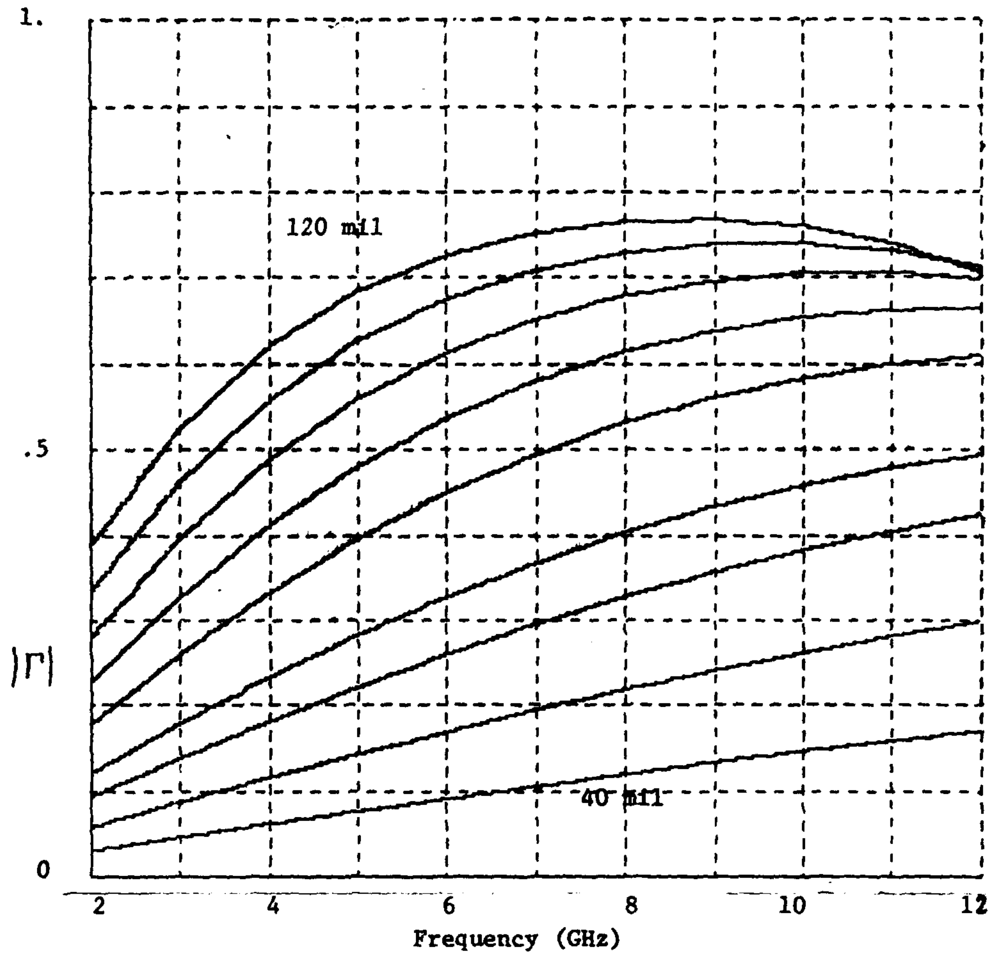

Fig. 5. Reflection Coefficient Magnitude for 40 to 120 mil Square METCHIPs (10 mil increments)

impedance transmission line, several METCHIPs were measured using an Automatic Network Analyzer (ANA).[3] The ANA System measures the 2-port scattering parameters of a microwave device. It automatically corrects for internal system errors using stored data from measured calibration standards. The METCHIPs were placed on a 50Ω microstrip line fabricated on a 25 mil alumina substrate, and measured at 9.35 GHz. The calculated and measured reflection coefficients are plotted on a portion of a Smith Chart in Fig. 7 for comparison. The measured values deviate from those calculated by -0.5 to -5.5% in magnitude. All the measured angles are rotated toward the generator (smaller reflection coefficient angle) by about 0.01 - 0.02 wavelengths. The reduction in magnitude may be caused by the small air gap between the METCHIP and the ceramic substrate. The angular rotation is due to fringing effects[3] at the interface of the METCHIP and the 50 ohm microstrip line. This effect can be accounted for by modifying the simple model to include short lengths of transmission line to shift the reference planes as shown in Fig. 8. The magnitude of this reference plane shift was empirically determined to be a linear function METCHIP width, i.e. $\Delta x = k(W - W_o)$. A best fit approximation to the measured values give $k \doteq 0.123$ and $W_o \doteq 24$ mils, where Δx, W_m and W_o are the physical lengths in mils, as indicated in Fig. 8. The results of this empirical correction to the transmission line model are shown by the dashed curve in Fig. 7. These results show that the modified transmission line model can be used to closely approximate the METCHIP performance. The reproducibility can be seen from the measured data in Fig. 7 for several devices which were remeasured after removal and replacement on the 50 ohm line.

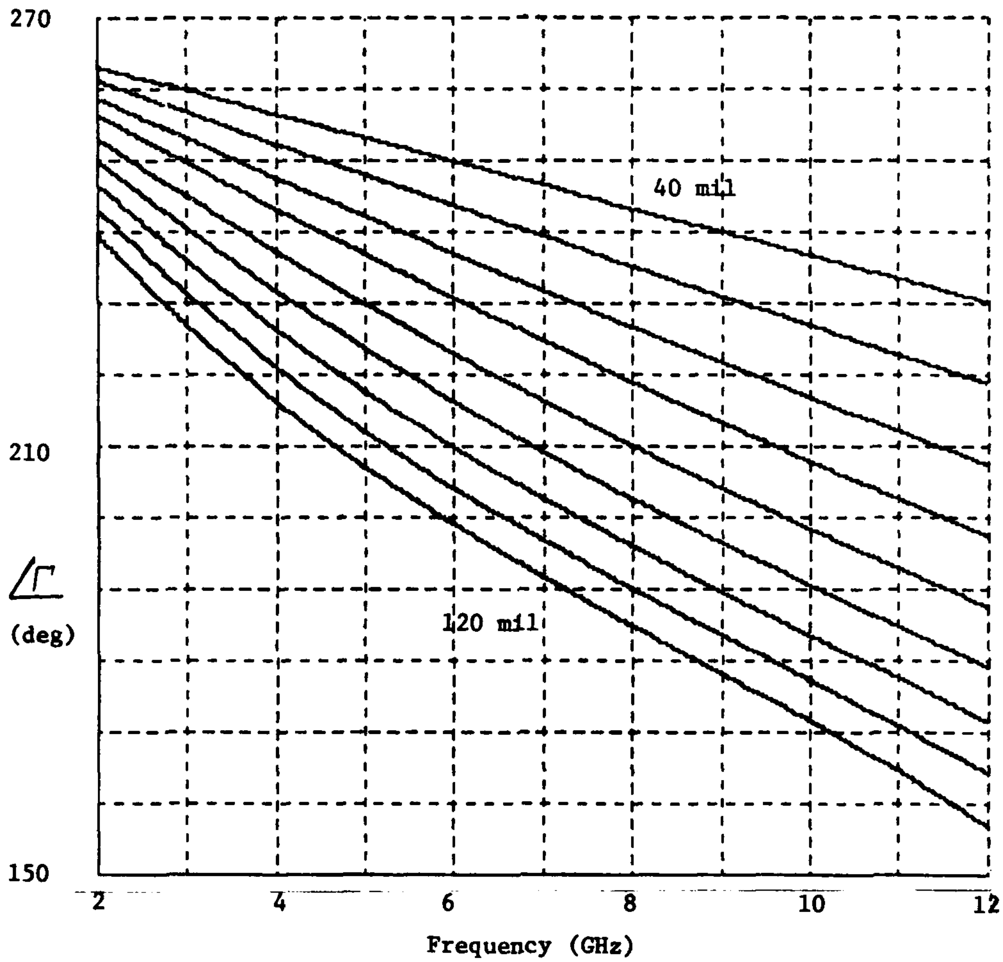

Fig. 6. Reflection Coefficient Angle for 40 to 120 mil METCHIPs (10 mil Increments)

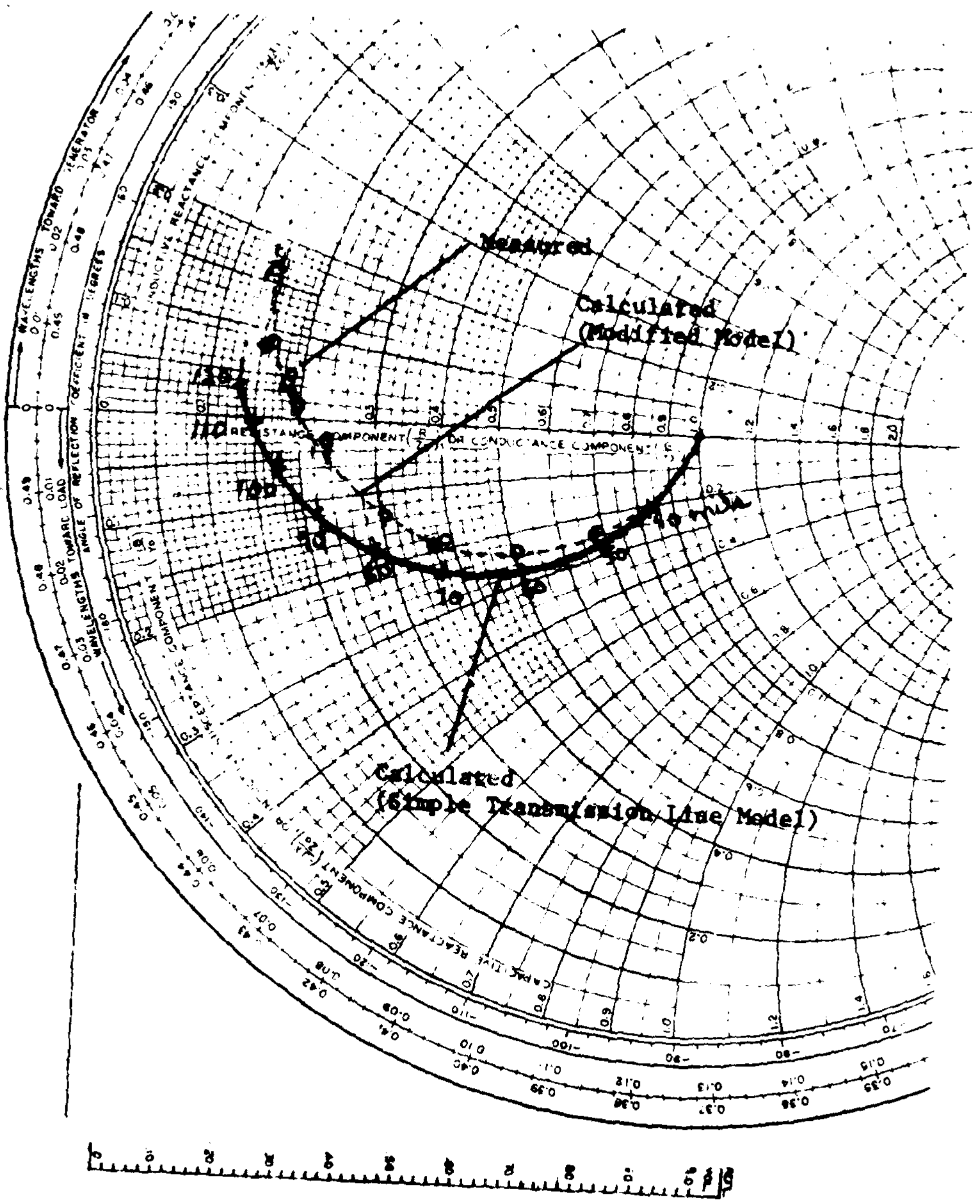

Fig. 7. Measured and Calculated Reflection Coefficients for METCHIPs at 9.35 GHz

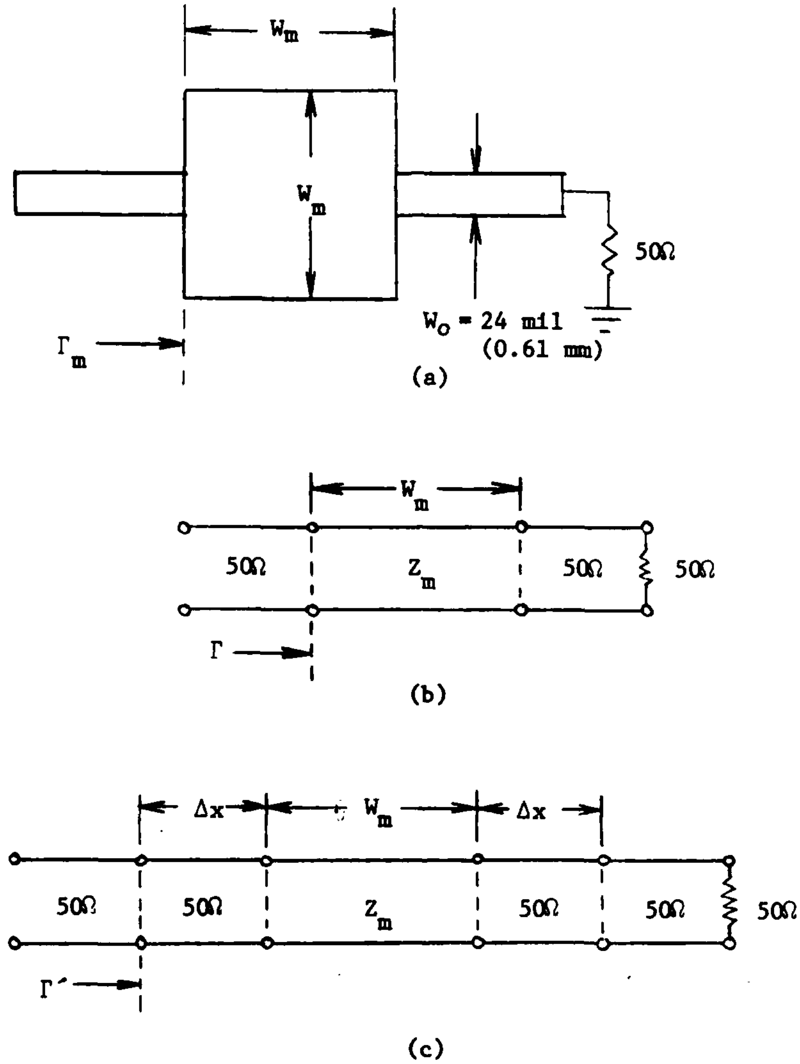

Fig. 8. (a) Physical Layout of METCHIP
(b) Simple Transmission Line Model
(c) Modified Transmission Line Model

II. APPLICATION TO MESFET MATCHING

A. The GaAs MESFET

The gallium arsenide metal epitaxial semiconductor field effect transistor, first proposed by Mead[18] in 1967, is establishing its performance superiority in most low noise microwave receiver designs. The GaAs FET is a unique device with numerous applications, for example: amplifiers, oscillators, mixers, modulators, parametric amplifier replacements, and RF switches. Demonstrated performance to date includes amplification at frequencies up to the millimeter-wave region (10 dB gain at 30 GHz), low noise amplification (less than 2 dB noise figure at 8 GHz), and more than 2 Watts power output at 10 GHz. This performance has opened the door to applications ranging from active-element phased array radars, to low-cost portable satellite receivers.

(1) Device Topology

Fig. 9 shows a plan and cross-sectional view of a typical GaAs MESFET. Alloyed metal ohmic contacts form the source and drain, and a metal-semiconductor (Schottky-barrier) junction forms the gate. High frequency performance is enhanced by the planar geometry, which minimizes stray capacitances, and by the high electron mobility of the gallium arsenide material, which is in the range of 3000 to 8000 cm^2/volt-sec at 300°C, about five times higher than silicon. The very short gate length, L_g, (0.2-2.0 microns) is a critical parameter, since it determines the electron transit time in the gate region, and therefore the maximum operating frequency. The saturated current I_{dss}, is proportional to the gate width, W_g, (approximately 300 microns in a low

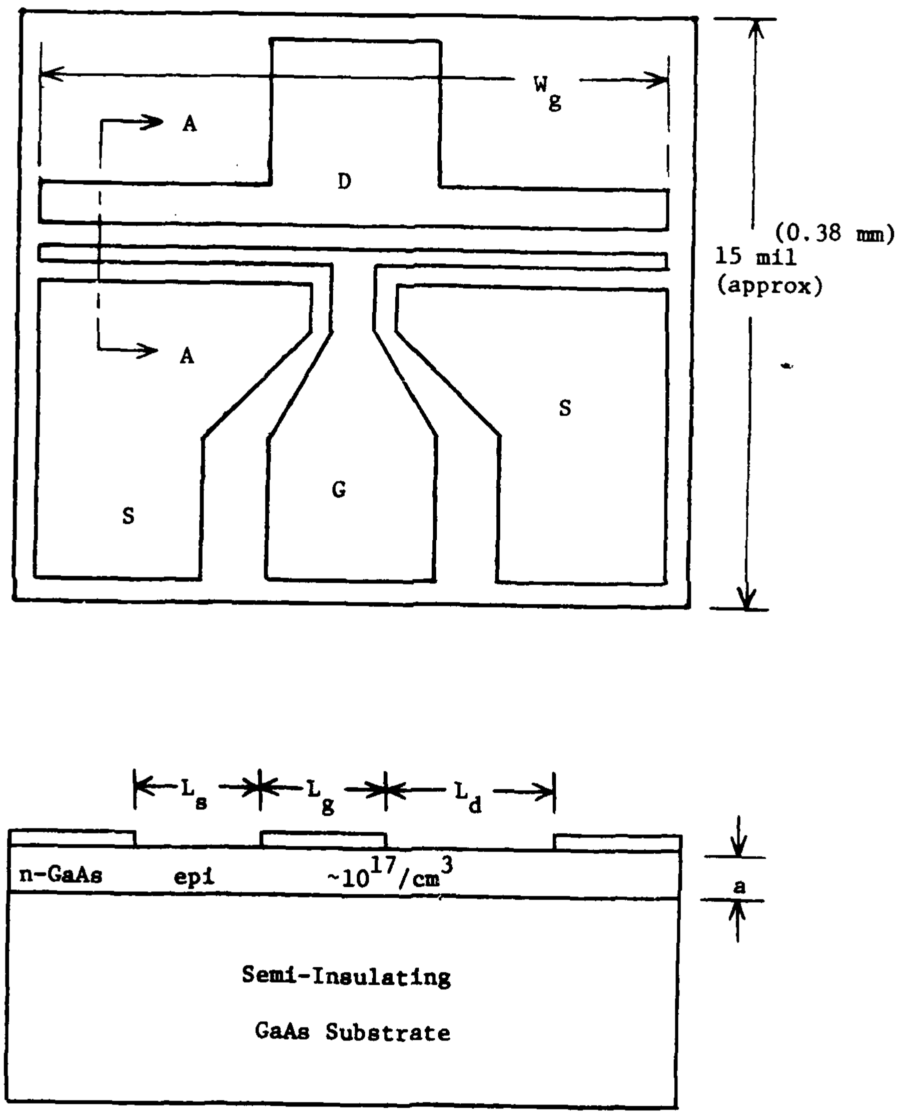

Fig. 9. MESFET Topology

noise device) and the active layer height, a, (0.1-1.0 microns), which therefore strongly influence the maximum power capability of the device.

(2) Equivalent Circuit

Fig. 10 shows the small signal lumped equivalent circuit elements of the GaAs MESFET in relation to the device geometry. The element values given are published results[4] based on device modelling of the type NEC244 transistor used in this investigation. Comparison of measured scattering parameters with those predicted by this model provide a useful check for the validity of the model.

B. Device Characterization Techniques

The noise figure and gain of a MESFET amplifier stage are functions of the source and load impedances, the device bias, the operating frequency, and the ambient temperature, humidity, and light level. Fortunately, the last three parameters have been seen to have only a small effect on most devices at room temperature, and under normal laboratory conditions. Measuring the effects of the first four parameters, however, still presents a formidable task, and requires a systematic approach to the device characterization.

(1) Measurement Setup

The setup diagrammed in Fig. 11 was designed to provide highly accurate gain and noise figure measurements for MESFET devices over the 8 to 10 GHz band. Frequency, bias, and tuning conditions can be changed and their effects measured without changing the setup configuration. Gain or noise figure measurements are selected by simultaneously energizing the two SPDT selenoid operated coaxial switches. Device tuning is accomplished directly on the FET test fixture using

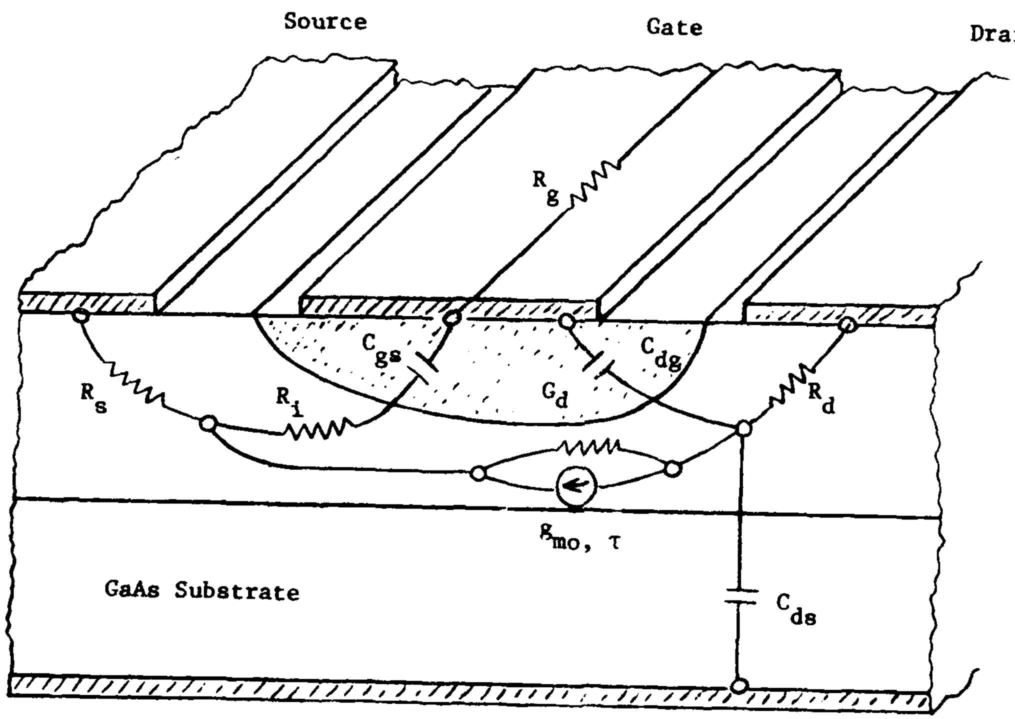

R_g = 4.8 ohm
R_s = 1.33 ohm
R_i = 0.97 ohm
R_d = 3.0 ohm
G_d = 1.67 mmho

g_{mo} = 18 mmho
C_{gs} = 0.35 pF
C_{dg} = .0039 pF
C_{ds} = 0.16 pF
τ = 4.2 psec

Fig. 10. Small Signal Lumped Equivalent Circuit of MESFET Based on Device Geometry

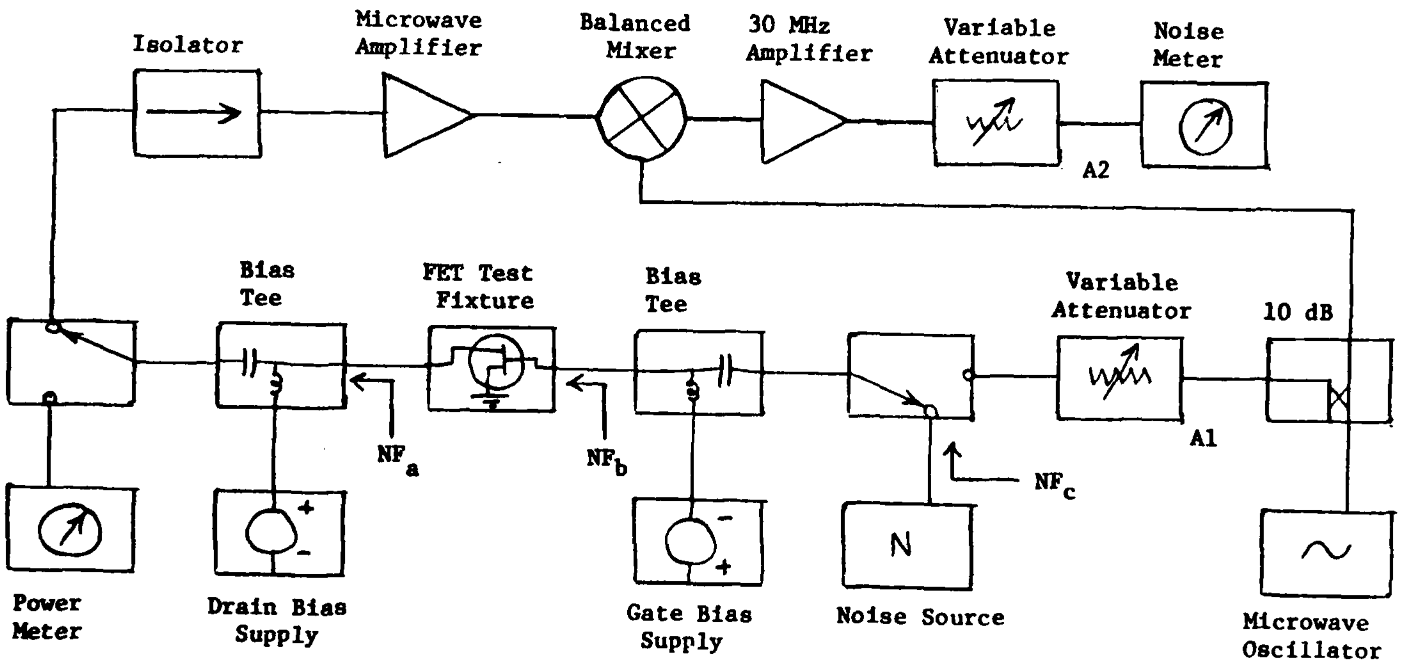

Fig. 11. Gain/Noise Figure Measurement Setup

METCHIPs, or with external coaxial tuners. The bias supplies incorporate series resistors of 100 ohms in the drain and 1000 ohms in the gate circuit provides "soft" bias to the device to avoid burnout due to bias supply transients. Independent monitoring of source and gate voltage and current is provided.

(2) Microstrip Test Fixture

The microstrip test fixture, sketched in Fig. 12, was designed specifically for MESFET microwave characterization, and is quite suitable for METCHIP tuning. As shown in Fig. 3, the FET die is mounted to a metal rib on the microstrip carrier using heat-setting epoxy adhesive. Thermocompression stitch-bonded 0.7 mil gold wires provide the device electrical connections. The device carrier is clamped into the test fixture assembly by tightening four screws which are tapped into the center block. This block is machined 5 mils shorter than the carrier to ensure good ground continuity. The center conductors of two miniature 50 ohm coaxial lines protrude from the end blocks to provide pressure contact to the microstrip lines. The coaxial sections then transition to precision, sexless 7 mm (type APC-7) connectors, which provide highly repeatable connections, and a precisely located reference plane.

(3) Gain/Noise Figure Measurement Procedure

To provide accurate measurements, the test setup of Fig. 11 must be calibrated at each measurement frequency, due to variations in loss, coupling, sweeper power output, and noise figure of system components over frequency. The calibration consists of the following steps:

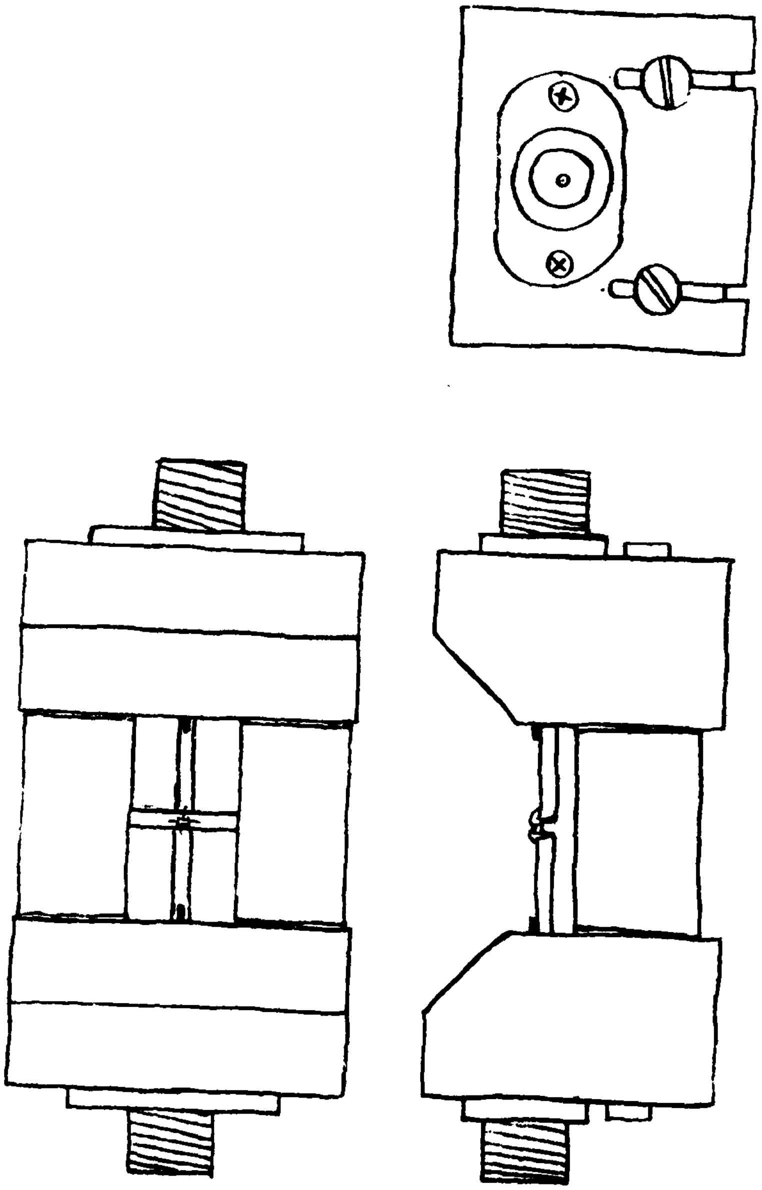

Fig. 12. Microstrip MESFET Test Fixture

1. Connect the microwave noise source to the drain bias tee. Measure and record the noise figure, NF_a, at each test frequency.

2. Replace the microstrip FET carrier with an equal length microstrip through line, connect the noise source to the test fixture, and measure the noise figure NF_b at each frequency.

3. Connect the setup in the standard configuration, and adjust variable attenuator, A1, for a standard reading on the microwave power meter at each frequency. (To ensure that gain measurements are made in the linear region of the FET device, the reference power level should be a minimum of 10 dB below the 1 dB device output gain compression level. For the NEC244 device, a reference level of 0.1 mW was used). Record the attenuator setting used at each frequency.

4. Measure and record the noise figure, NF_c, at each frequency.

After the setup has been calibrated, the microstrip FET carrier can be replaced into the test fixture and measurements taken without further calibration. It was found that the setup calibration would hold without significant drift for at least eight hours, however it should be recalibrated if measurements are made on a subsequent day.

Measurement of device gain is straight-forward. Since all signal losses are accounted for in the setup calibration, the device gain is simply $G_d = P_{measured}/P_{ref}$.

Finding the device noise figure, NF_d, from the measured noise figure, NF_m, requires a knowledge of the loss between the noise source and the device, L_1, and the noise figure of the system following the device, NF_2. Recalling that the noise figure of a linear, passive

element at room temperature is equal to its insertion loss, the loss of the microstrip test fixture is simply: $L_f = NF_b - NF_a$, where quantities are expressed in dB. Since the fixture is symmetrical, it can be assumed that this loss is split between the input and output ports of the fixture. The required quantities L_1 and NF_2 can now be determined where $NF = 10 \log F$ as:

$$L_1 = NF_c - NF_b + (NF_b - NF_a)/2 \tag{7}$$

$$\text{and } NF_2 = NF_a + (NF_b - NF_a)/2, \tag{8}$$

where all quantities are expressed in dB. Now, using the Friis equation for cascaded noisy 2-ports:

$$F_{TOT} = F_1' + (F_2' - 1)/G_1' + (F_3' - 1)/G_1'G_2' + \cdots, \tag{9}$$

where all quantities are expressed as ratios, the measured noise figure can be related to the device noise figure by:

$$\begin{aligned} F_m &= L_1 + (F_d - 1)L_1 + (F_2 - 1)L_1/G_d \\ &= L_1\ (F_d + (F_2 - 1)/G_d). \end{aligned} \tag{10}$$

As this equation clearly shows, the measured noise figure value is a function of both the device gain and noise figure. In order to converge on a bias or tuning condition that results in a minimum device noise figure, the actual value of NF_d must be determined for each subsequent adjustment. This can be done with either a programmable calculator, or by using a family of curves such as those plotted in Fig. 12a. This plot was used to quickly estimate the device noise figure from the measured data, for a system calibration at 9.35 GHz,

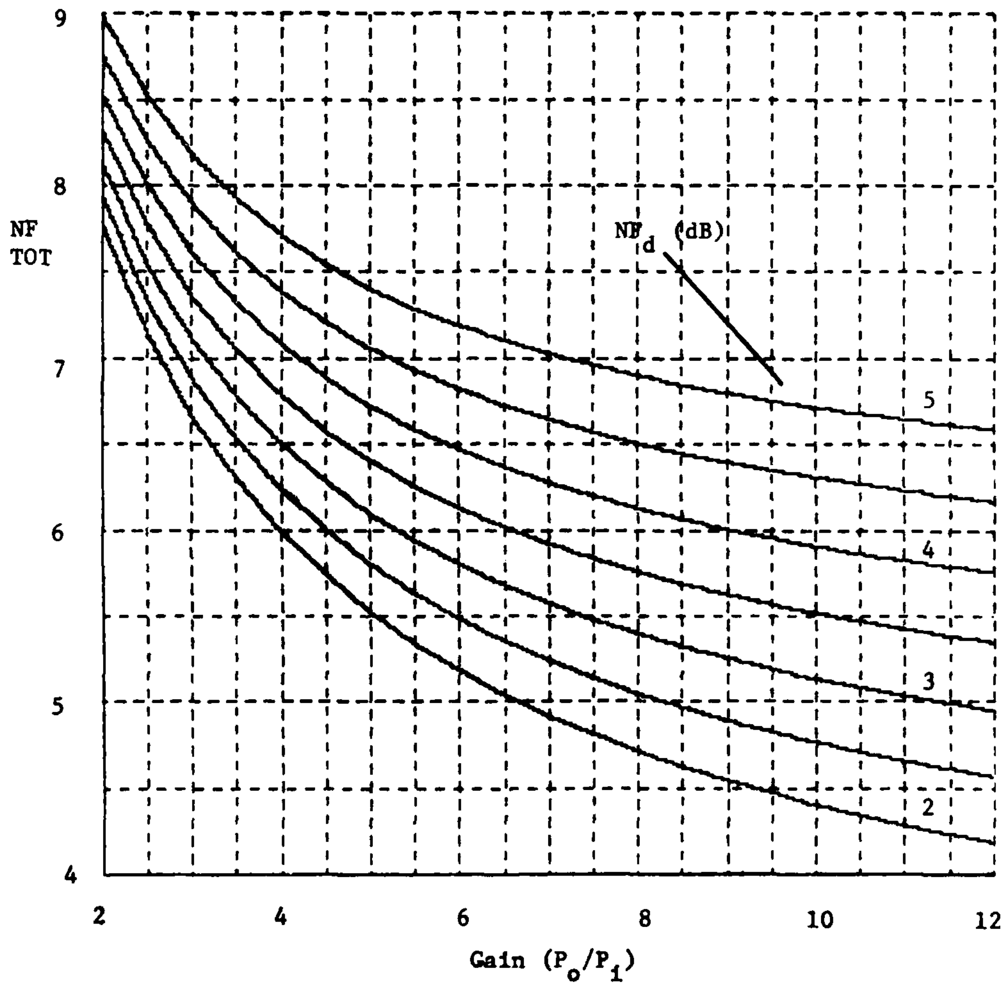

Fig. 12a. Graph Used to Find Device Noise Figure from Measured Noise Figure and Gain (L_1 = 0.9 dB, NF_2 = 8.8 dB) From Measurements Described in Eqns. 7 and 8.

where $L_1 = 0.9$ dB and $NF_2 = 8.8$ dB.

C. MESFET Characterization

The type NEC 244 MESFET was selected for this investigation, since it is well known and widely used in the microwave industry. It is a one-micron gate length, 300 micron gate width device designed for low noise applications at frequencies up to 12 GHz.

(1) Effect of Device Bias

Selecting a suitable bias point for a low noise amplifier stage requires a knowledge of the tuned minimum noise figure and associated device gain over a wide range of bias conditions. The initial measurements showed that while drain voltage variation showed a small effect, the drain current level was by far the determining parameter for the device noise figure and gain. The drain voltage was therefore fixed at 3 V to remain in the saturated drain current region of the device, and below the nominal 6 V gate-to-drain breakdown voltage for the range of applied gate bias. The drain current was adjusted to values from 2.5 to 35 mA by controlling the gate voltage. At each value of drain current, the MESFET was tuned for the minimum device noise figure using a coaxial tuner at the input, and METCHIP tuning at the output of the device. The measured results, shown in Fig. 13, indicate that the optimum bias levels for low noise figure and high gain show conflicting trends. To determine a suitable bias level for low noise operation, a quality factor called noise measure, M, can be defined as the noise figure of an infinite cascade of identical amplifier stages. Solving the Friis equation for this condition gives:

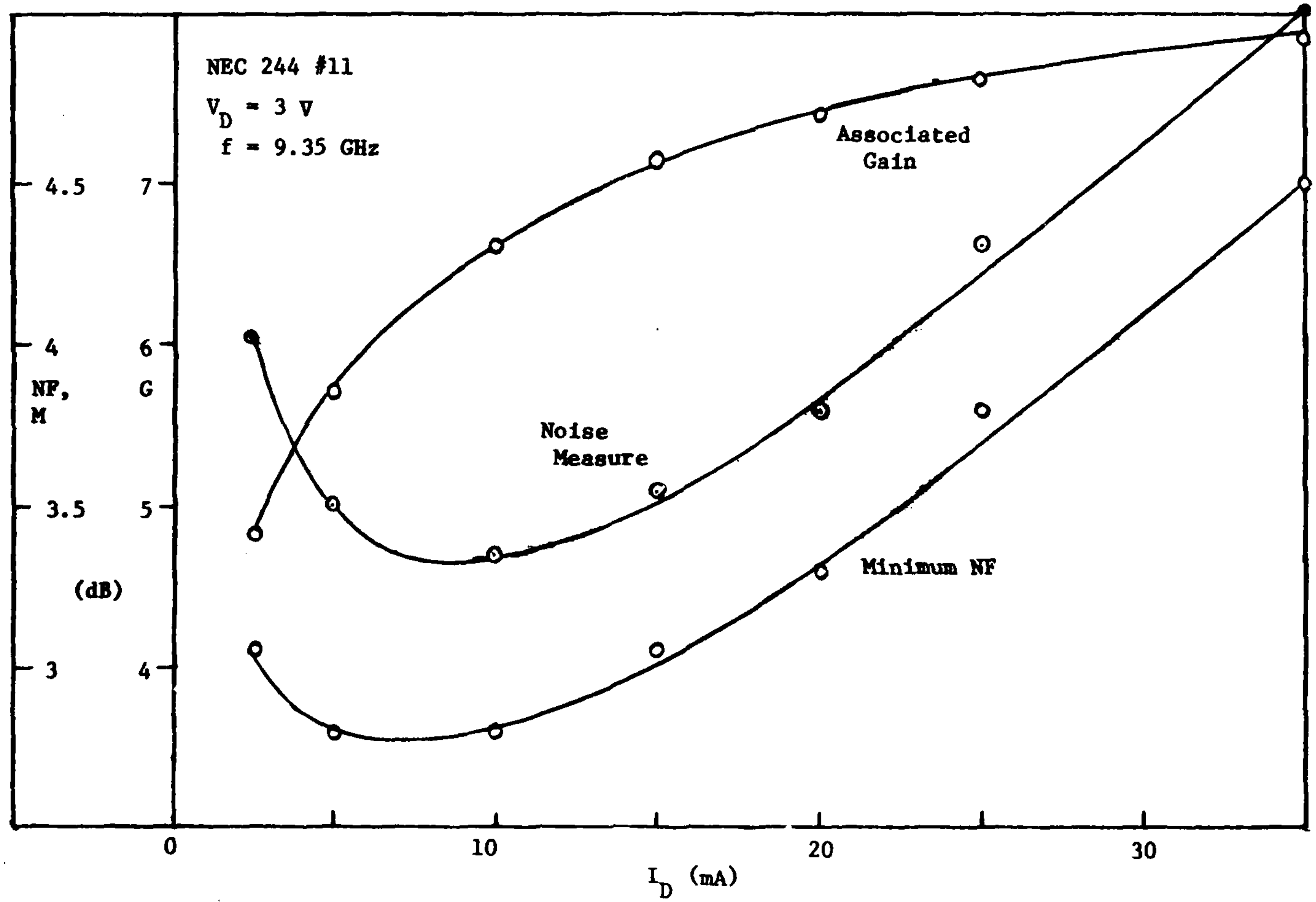

Fig. 13. Noise Figure and Gain Versus Drain Current for MESFET

$$M = F + \frac{F-1}{G} + \frac{F-1}{G^2} + \cdots$$
$$= (FG-1)/(G-1) \qquad (11)$$

where quantities are expressed as ratios. From Fig. 13, the optimum noise measure of 3.34 dB occurs at a drain bias level of about 10 ma. The bias was fixed at this point ($V_D = 3$ V, $I_D = 10$ mA) for the subsequent measurements.

(2) Noise Figure Variation with Tuning

To understand the noise figure behavior of a GaAs FET stage due to tuning variations, it is fruitful to refer to the analysis of Haus and Adler,[5] in which the transistor is treated as a noisy linear two-port network. The analysis shows that the noise figure can be expressed as a function of the source admittance by the relation:

$$F = F_{min} + R_n/G_s[(G_s - G_{on})^2 + (B_s - B_{on})^2], \qquad (12)$$

F_{min} = minimum device noise figure

R_n = equivalent noise resistance of device

$G_{on} + jB_{on}$ = optimum source admittance for F_{min}

$G_s + jB_s$ = actual source admittance

In terms of the source reflection coefficient, this can be expressed as:

$$F = F_{min} + 4R_n \frac{|\Gamma_s - \Gamma_{on}|^2}{(1 - |\Gamma_s|^2)|1 + \Gamma_{on}|^2} \qquad (13)$$

The parameter R_n is found to be:

$$R_n = (F_o - F_{min})(|1 + \Gamma_{on}|^2/4|\Gamma_{on}|^2) \qquad (14)$$

where F_o = noise figure where $\Gamma_s = 0$.

For a given frequency, bias, and output tuning, a unique set of parameters F_{min}, F_o and Γ_{on} can be obtained using the measurement setup. It was found that the output tuning produced a negligible effect on these noise parameters as long as it was adjusted near the optimum gain point. This is expected due to the high reverse isolation (small value of S_{12}) of the GaAs FET device. The following procedure was used to measure the noise parameters:

1. Adjust the device bias point near the optimum noise measure condition. (For the NEC 244 GaAs FET, $V_D = 3$ V, I_D = 10 mA).

2. With the input unmatched, ($\Gamma_s = 0$), adjust the output tuning using an appropriate METCHIP to obtain maximum gain.

3. Measure the resulting gain and noise figure and calculate the device noise figure, NF_o, using the Friis equation, or the family of noise curves.

4. Adjust the input tuning using an appropriate METCHIP to obtain a minimum device noise figure, NF_{min}.

5. Measure the length of transmission line, x, between the input tuning METCHIP and the MESFET using a low power microscope with a calibrated reticle, and calculate Γ_{on} using the relation:

$$\Gamma' = \Gamma e^{-j2kx}, \text{ where } k = 2\pi f\sqrt{\epsilon_r'}/c, \qquad (15)$$

ϵ_r' = effective dielectric constant of the 50 ohm microstrip line.

Performing the above procedure for the NEC 244 MESFET at 9.35 GHz produced measured values of NF_o = 3.50 dB, NF_{min} = 2.81 dB

using an 80 mil METCHIP with x = 67 mils. From Fig. 7 it is seen that the measured reflection coefficient of the 80 mil METCHIP is $0.54\underline{/196°}$. Transforming through the distance x to the MESFET input terminals produce a phase shift of $\Delta\phi$ = -2kx radians

$$= -2(360)\ fx\sqrt{\varepsilon_r}/c \text{ deg}$$

$$= -61.9 \cdot f(\text{GHz}) \cdot x(\text{cm}) \text{ deg}$$

$$= -98 \text{ deg for } x = 67 \text{ mils, } f = 9.35 \text{ GHz}$$

Then $\Gamma_{on} = 0.54\ \underline{/196-98°} = 0.54\underline{/98°}$.

The device noise figure for any input tuning condition, Γ_s, can now be found from these noise parameters and Eqn's 13 and 14. This can be shown graphically by constructing a family of "noise figure circles" on the Smith Chart of the Γ_s plane. The circles have centers and radii calculated by Haus and Adler to be:

$$\text{center:}\quad C_i = \Gamma_{on}/(1 + N_i) \tag{16}$$

$$\text{radius:}\quad R_i = \sqrt{N_i^2 + N_i(1 - |\Gamma_{on}|^2)}/(1 + N_i) \tag{17}$$

$$\text{where}\quad N_i = (F_i - F_{min})|1 + \Gamma_{on}|^2/4R_n \tag{18}$$

F_i is the noise figure that results from any source reflection coefficient on the locus of the circle. C_i and R_i were calculated for values of $NF_i = NF_{min}$ + 0.10, 0.25, 0.5 and 1.0 dB. The results are plotted in Fig. 14.

(3) Device Scattering Parameters/Gain versus Tuning

The scattering parameters of the NEC 244 FET were measured with the device mounted in the 50 Ω microstrip test fixture previously

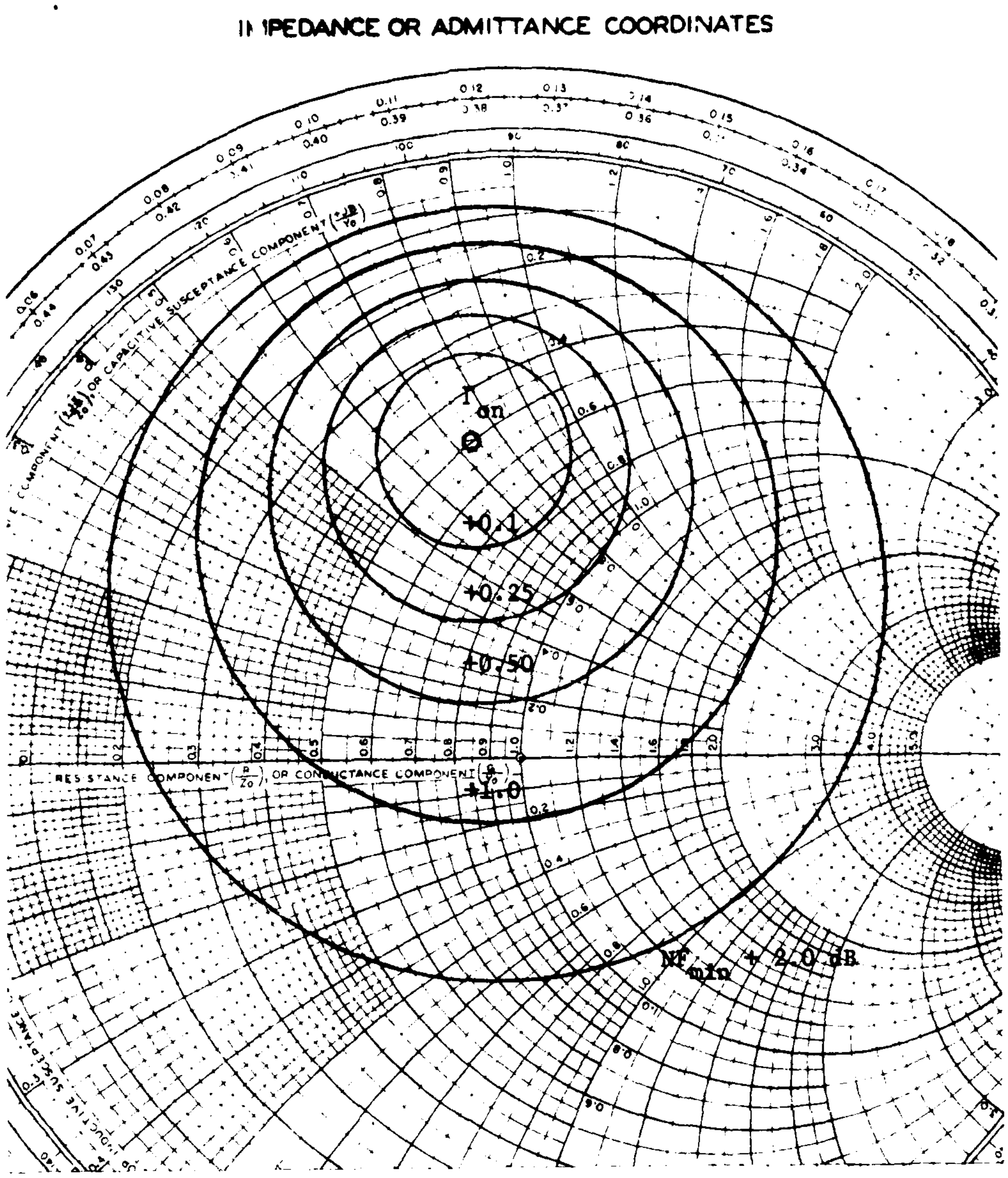

NF_{min} = 2.81 dB

Fig. 14. Noise Figure Versus Input Tuning NEC 244, V_D = 3 V, I_D = 10 mA, f = 9.35 GHz

described. The device was biased at $I_D = 10$ mA, $V_D = 3$ V, and the S-parameters measured over the 8 to 10 GHz range using an Automatic Network Analyser. The results are given in Table 3.

Using the two-port power flow analyzer of Bodway,[6] the small signal gain, stability, and input and output reflection coefficients of a FET amplifier stage can be predicted from the measured S-parameters, for any assumed source and load impedance condition. From Bodway's analysis, the maximum available power gain of the device is given by:

$$G_{amax} = |S_{21}/S_{12}|^2 |K \pm \sqrt{K^2-1}| \tag{19}$$

$$\text{where:} \quad K = \frac{1 + |\Delta|^2 - |S_{11}|^2 - |S_{22}|^2}{2|S_{21}||S_{12}|} \tag{20}$$

$$\text{and:} \quad \Delta = S_{11}S_{22} - S_{12}S_{21} \tag{21}$$

This gain is achieved for simultaneous conjugate matching of the device. The source and load reflection coefficients required for conjugate match are given by:

$$\Gamma_{ms} = C_1^* \frac{B_1 \pm \sqrt{B_1^2 - 4|C_1|^2}}{2|C_1|^2} \tag{22}$$

$$\Gamma_{ml} = C_2^* \frac{B_2 \pm \sqrt{B_2^2 - 4|C_2|^2}}{2|C_2|^2} \tag{23}$$

$$B_1 = 1 + |S_{11}|^2 - |S_{22}|^2 - |\Delta|^2 \tag{24}$$

$$B_2 = 1 + |S_{22}|^2 - |S_{11}|^2 - |\Delta|^2 \tag{25}$$

PAGE 1: 27 SEPT 1978

GaAs FET CHARACTERIZATION

NEC244 #16 ID = 10 MA; VDS = 3 V

.00 VOLTS, .00 MA (MEAS 1) NEC244-16 10MA/3V

FREQ	S11		S21		S12		S22	
(MHZ)	MAG	ANG	MAG	ANG	MAG	ANG	MAG	ANG
8000.000	.721	-82	1.484	100	.062	56	.793	-22
8200.000	.709	-84	1.510	96	.064	54	.801	-22
8400.000	.697	-88	1.542	94	.063	55	.780	-19
8600.000	.670	-92	1.566	91	.065	53	.777	-18
8800.000	.674	-100	1.589	88	.067	50	.773	-19
9000.000	.639	-105	1.599	85	.067	49	.747	-20
9200.000	.642	-108	1.627	85	.071	49	.746	-17
9350.000	.656	-114	1.582	83	.069	48	.709	-20
9400.000	.637	-115	1.543	82	.070	46	.712	-22
9600.000	.646	-116	1.560	82	.073	46	.692	-24
9800.000	.644	-121	1.556	80	.075	44	.688	-29
10000.00	.650	-124	1.493	79	.076	42	.680	-33

Table 3. NEC 244 MESFET Scattering Parameters

$$C_1 = S_{11} - \Delta S_{22}^* \qquad (26)$$

$$C_2 = S_{22} - \Delta S_{11}^* \qquad (27)$$

(The plus sign of Eqns 19, 22 and 23 is used if K, $B_i < 0$, and minus if K, Bi > 0.)

The device is unconditionally stable for all tuning conditions of $|\Gamma_s|$, $|\Gamma_L| < 1$, if $K > 1$ and B_1, $B_2 > 0$.

If port 1 is not conjugately matched, the available gain G_a can be expressed as a function of the source reflection coefficient Γ_s by:

$$\frac{1}{G_a} = \frac{1}{G_{a_{max}}} + \frac{4\,\mathrm{Reg}|\Gamma_s - \Gamma_{ms}|^2}{(1 - |\Gamma_s|^2)|1 + \Gamma_{ms}|} \qquad (28)$$

Using this relation, a family of constant gain circles can be plotted on a Smith Chart in the source reflection coefficient plane. These circles will have centers C_{Gi} and radii R_{Gi} given by:

$$C_{Gi} = \Gamma_{ms}/(1 + G_{ai}) \qquad (29)$$

$$R_{Gi} = (1/(1 + G_{ai}))\sqrt{G_{ai}^{\,2} + G_{ai}\,(1 - |\Gamma_{ms}|^2)} \qquad (30)$$

$$G_{ai} = \frac{1}{G_a} - \frac{1}{G_{amax}} \quad \frac{|1 + \Gamma_{ms}|^2}{4\,R_{eg}} \qquad (31)$$

$$R_{eg} = R_e\,(y_{22})/|y_{21}|^2 \qquad (32)$$

$$y_{22} = \frac{(1 + S_{11})(1 - S_{22}) + S_{21}S_{12}}{(1 + S_{11})(1 + S_{22}) - S_{21}S_{12}} \qquad (33)$$

$$y_{21} = \frac{-2S_{21}}{(1 + S_{11})(1 + S_{22}) - S_{21}S_{12}} \qquad (34)$$

Similar relations for the available gain, due to variations in the load reflection coefficient Γ_L, can be obtained by exchanging S_{11} with S_{22} and S_{12} with S_{21} in the above relations.

To determine the effect of input and output tuning on the gain of the FET amplifier stage, a program was written in BASIC to perform the complex arithmetic to evaluate equations 19 to 34, and to plot families of gain circles in the source and load reflection coefficient planes. The program is listed in Table 4. A sample execution is shown in Figs. 15 and 16 for the NEC 244 FET at 9.35 GHz. Outputs for S-parameters in the 8 to 10 GHz range are listed in Table 5.

The gain circles clearly illustrate the sensitivity of the gain to the source and load reflection coefficient values. It can be seen from Figs. 15 and 16 that the coefficients must be controlled to within approximately ±25% in amplitude and 20° in phase to obtain a value of gain within 2 dB of the maximum available.

D. Low Noise MESFET Amplifier

Using the procedures outlined in Sections IIB and C, the NEC 244 FET was tuned using METCHIP matching for optimum noise figure at 9.35 GHz. The physical layout and electrical equivalent circuits for the amplifier stage are shown in Fig. 17. The measured METCHIP positions are $x_1 = 54$ mils and $x_2 = 98$ mils. The equivalent free space electrical line lengths ℓ_1 to ℓ_4 for the circuit model are:

```
S11 (MAG,ANG) = .656083        -113.999
S12 (MAG,ANG) = 6.89965E-02     47.9939
S21 (MAG,ANG) = 1.58211        82.9977
S22 (MAG,ANG) = .700996        -19.9949
K = 1.39243
RHO(MS) (MAG,ANG) = .729107       127.572
RHO(ML) (MAG,ANG) = .772028       30.1651
R(EG) = 2.89708E-02
G(MAX) = 9.87234      dB
----
```

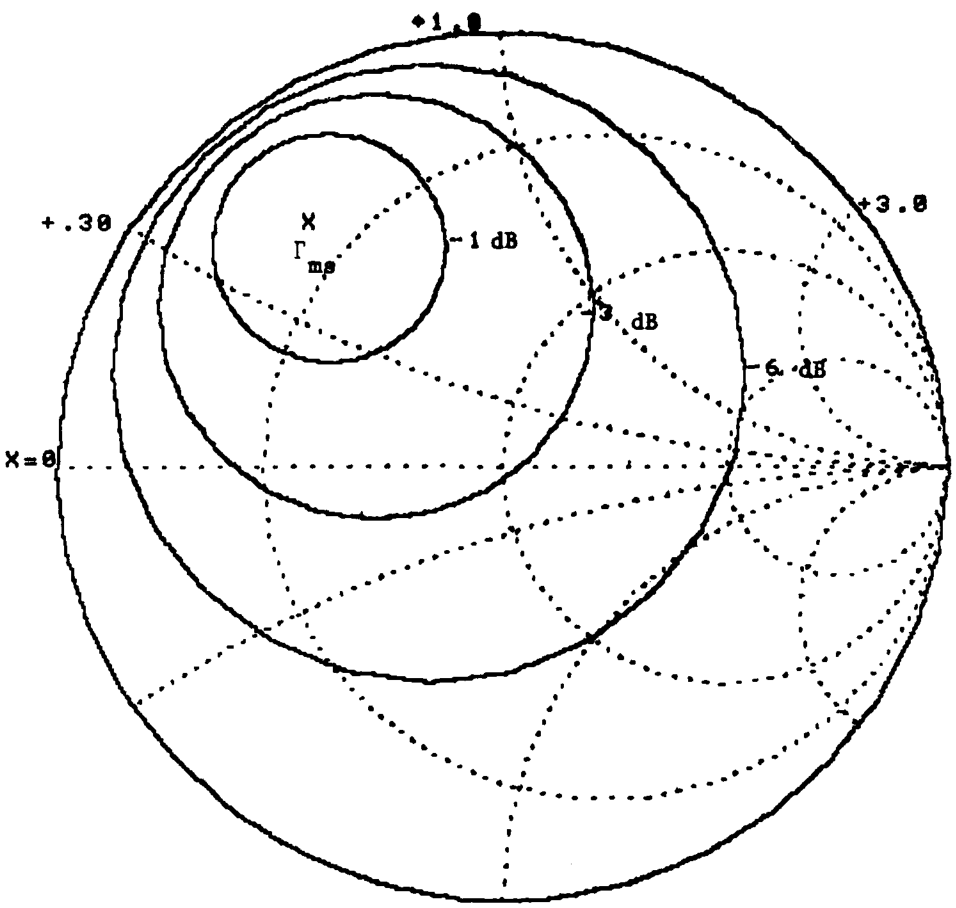

Fig. 15. Constant Gain Circles in the Input Reflection Coefficient, Γ_s, Plane

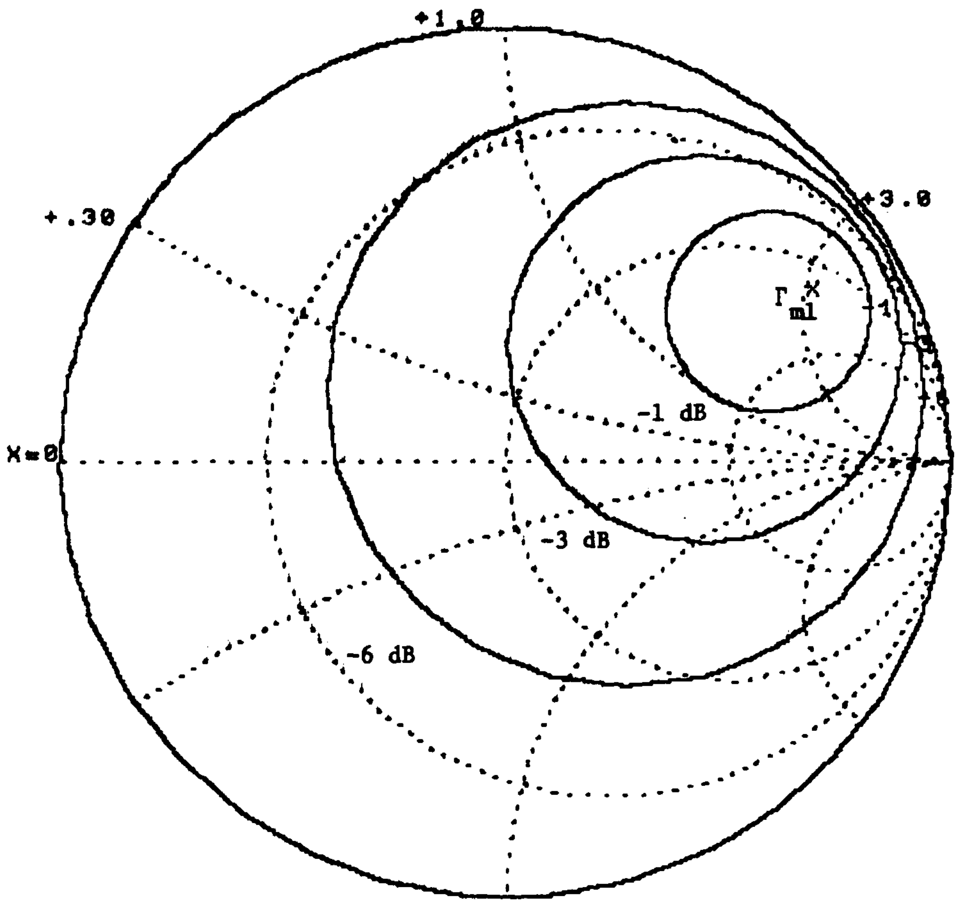

Fig. 16. Constant Gain Circles in the Output Reflection Coefficient, Γ_L, Plane

Program to calculate the optimum source impedance and load impedance ,RHO(MS) & RHO(ML), and plot gain circles when the device S-parameters are given.

```
5   DATA .551,-132
6   DATA .126,34
7   DATA 1.568,65
8   DATA .636,-37
10  DIM S[12]
15  CLEAR(1)
20  LET N=0
30  FOR L=1 TO 2
40  FOR M=1 TO 2
60  LET N=N+1
65  DSPLAY "S";L;M;"(MAG,ANG) = ";
70  INPUT A,B
75  LET B=B/57.296
80  CPAK(A*COS(B),A*SIN(B),S[N])
90  NEXT M
100  NEXT L
104  CLEAR(1)
105  DSPLAY "S11 (MAG,ANG) = ";MAG(S[1]);ANG(S[1])
106  DSPLAY "S12 (MAG,ANG) = ";MAG(S[2]),ANG(S[2])
107  DSPLAY "S21 (MAG,ANG) = ";MAG(S[3]);ANG(S[3])
108  DSPLAY "S22 (MAG,ANG) = ";MAG(S[4]);ANG(S[4])
110  CMPY(S[1],S[4],S1)
120  CMPY(S[2],S[3],S2)
130  CSUB(S1,S2,D)
140  LET K=1+MAG(D)↑2-MAG(S[1])↑2-MAG(S[4])↑2
150  LET K=K/(2*MAG(S[3])*MAG(S[2]))
155  DSPLAY "K = ";K
156  IF K>1 GOTO 160
157  DSPLAY "CONITIONALLY STABLE S-PARAMETERS"
158  STOP
160  LET B=MAG(S[1])↑2-MAG(S[4])↑2
170  LET B1=1+B-MAG(D)↑2
180  LET B2=1-B-MAG(D)↑2
190  CPAK(REA(S[4]),-IMG(S[4]),S3)
200  CMPY(S3,D,S4)
210  CSUB(S[1],S4,C1)
220  CPAK(REA(S[1]),-IMG(S[1]),S5)
230  CMPY(S5,D,S6)
240  CSUB(S[4],S6,C2)
250  LET R1=B1-SQR(B1↑2-4*MAG(C1)↑2)
260  LET R1=R1/(2*MAG(C1)↑2)
270  CPAK(REA(C1),-IMG(C1),C3)
280  CPAK(R1,0,R1)
290  CMPY(R1,C3,R1)
295  DSPLAY "RHO(MS) (MAG,ANG) = ";MAG(R1);ANG(R1)
300  LET R2=B2-SQR(B2↑2-4*MAG(C2)↑2)
```

Table 4. GAIN CIRCLES - Program Listing

```
310  LET R2=R2/(2*MAG(C2)↑2)
320  CPAK(REA(C2),-IMG(C2),C4)
330  CPAK(R2,0,R2)
340  CMPY(R2,C4,R2)
345  DSPLAY "RHO(ML)  (MAG,ANG)  =  ";MAG(R2);ANG(R2)
350  CPAK(1,0,U)
360  CADD(U,S[1],S5)
370  CADD(U,S[4],S6)
380  CSUB(U,S[4],S7)
390  CMPY(S5,S6,S8)
400  CSUB(S8,S2,S8)
410  CMPY(S5,S7,S9)
420  CADD(S9,S2,S9)
430  CDIV(S9,S8,S9)
440  LET R=REA(S9)
450  CPAK(-2*REA(S[3]),-2*IMG(S[3]),S5)
460  CDIV(S5,S8,S5)
470  LET R=R/(MAG(S5)↑2)
480  DSPLAY "R(EG) = ";R
500  LET G=K-SQR(K↑2-1)
510  LET G=G*MAG(S[3])/MAG(S[2])
515  LET G4=4.3429*LOG(G)
516  DSPLAY "G(MAX) = ";G4;"dB"
517  PAUSE
518  CLEAR(1)
520  CADD(U,R1,G1)
530  LET G1=MAG(G1)↑2/(4*R*G)
540  BUF(75)
555  SCALE(-1,1,-1,1)
556  PLOT(REA(R1),IMG(R1),3)
557  LABEL "X"
560  FOR N=1 TO 5 STEP 2
565  IF N>3 LET N=6
570  LET G2=G1*(1.2589↑N-1)
580  LET R3=SQR(G2↑2+G2*(1-MAG(R1)↑2))/(1+G2)
590  LET X=REA(R1)/(1+G2)
600  LET Y=IMG(R1)/(1+G2)
605  LET Q=0
610  FOR M=0 TO 24
615  IF M>0 LET Q=3
620  LET S=3.14159*M/12
630  PLOT(X+R3*COS(S),Y+R3*SIN(S),Q)
640  NEXT M
645  LABEL "-"N
650  NEXT N
660  SMITH(1,1)
```

Table 4. (Continued)

F (GHz)	K	G_{amax} (dB)	Γ_{ms} (mag, ang)	Γ_{mL} (mag, ang)
8.0	1.11	11.75	0.84, 98	0.89, 32
8.4	1.18	11.29	0.79, 105	0.86, 29
8.8	1.20	11.03	0.77, 118	0.84, 29
9.2	1.28	10.43	0.73, 126	0.81, 27
9.6	1.41	9.51	0.72, 129	0.76, 34
10.0	1.36	9.33	0.76, 136	0.78, 43

Table 5. Calculated Stability Factor, Optimum Gain, and Optimum Matching for NEC 244 FET

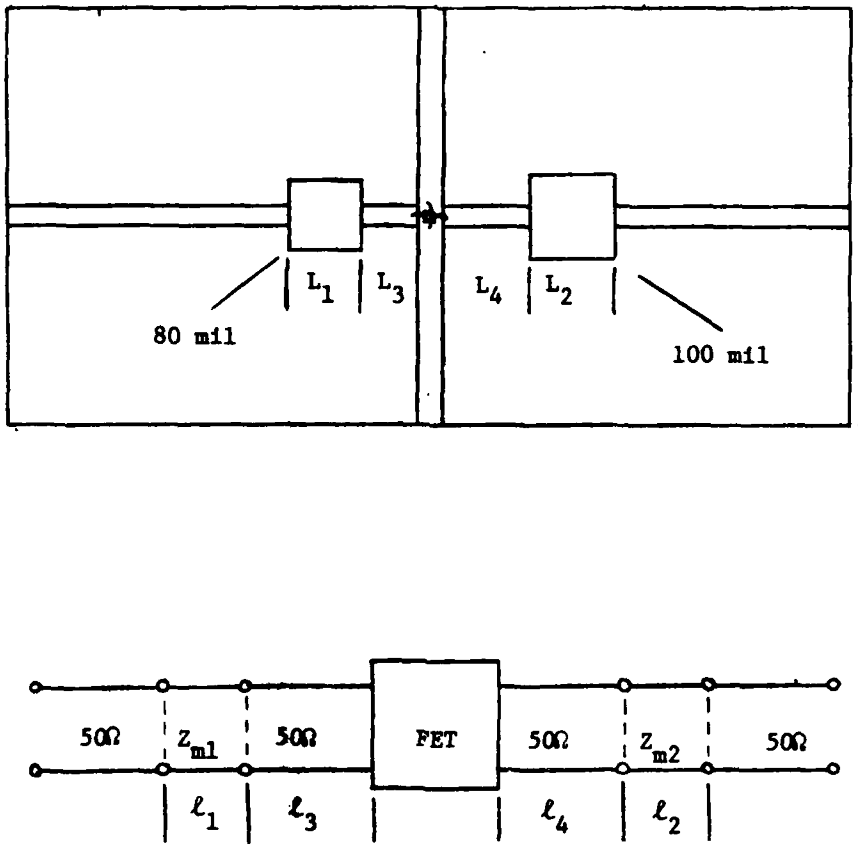

Fig. 17. FET Amplifier Stage

(a) Physical Layout (5 X scale)
(b) Electrical Equivalent Circuit

$$\ell_1 = L_1\sqrt{\varepsilon_{r1}} \tag{35}$$

$$\ell_2 = L_2\sqrt{\varepsilon_{r2}} \tag{36}$$

$$\ell_3 = (L_3 + \Delta x_1)\sqrt{\varepsilon_{ro}} \tag{37}$$

$$\ell_4 = (L_4 + \Delta x_2)\sqrt{\varepsilon_{ro}} \tag{38}$$

where ε_{r1}, ε_{r2}, and ε_{ro} are the effective relative dielectric constants of the 80, 100, and 24 mil width microstrip lines, and Δx_1, Δx_2 are the lengths given by the modified METCHIP model of Chapter I. Z_{m1} and Z_{m2} are obtained from Table 1 as 24.4 and 20.8 ohms, respectively.

Fig. 18 shows the amplifier performance measured on the gain/noise figure test setups over the 8 to 10 GHz range. The plotted values represent the overall amplifier stage performance, and are not corrected for circuit losses. These measurements show that one can obtain a good noise figure and gain match over a moderate bandwidth at X-band using the METCHIP matching technique.

III. COMPARISON TO CIRCUIT MODEL

In this chapter, the NEC 244 MESFET is modeled as a small signal lumped-element equivalent circuit. The FET model is inserted into the FET amplifier circuit model of Fig. 17, and the predicted performance is compared with the actual measured results.

A. GaAs MESFET Model and Analysis

An equivalent circuit model which has been shown to be useful

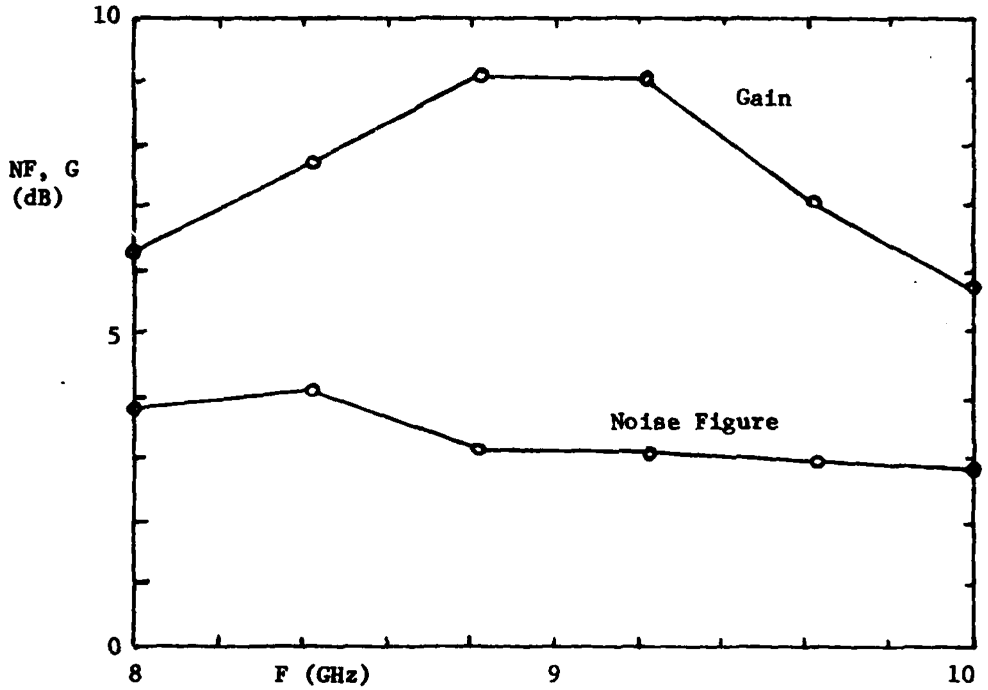

Fig. 18. Noise Figure and G are of Low Noise MESFET Amplifier Stage

in predicting small-signal MESFET behavior[4] is shown in Fig. 18. In order to predict the S-parameters in a 50Ω system, source and load generators E_1, R_1 and E_2, R_2 were added to the FET model. A program was written in BASIC to analyze this circuit, given the lumped element values and the frequency, and to output the S-parameters of the model.

The program solves three simultaneous equations to determine the loop currents I_1, I_2, and I_3 for the two conditions $E_1 = 1$, $E_2 = 0$ and $E_1 = 0$, $E_2 = 1$. The scattering parameters are determined from the currents I_1 and I_2 as follows:

By definition, the incident waves a_1, a_2 and the reflected waves b_1, b_2 are related by the scattering parameters as:

$$b_1 = S_{11}a_1 + S_{12}a_2 \qquad (39)$$

$$b_2 = S_{21}a_1 + S_{22}a_2 \qquad (40)$$

where,

$$a_n \equiv \tfrac{1}{2}(V_n/\sqrt{Z_{cn}} + \sqrt{Z_{cn}}\, I_n) \qquad (41)$$

$$b_n \equiv \tfrac{1}{2}(V_n/\sqrt{Z_{cn}} - \sqrt{Z_{cn}}\, I_n) \qquad (42)$$

Now, letting $Z_{cn} = 50\ \Omega$, and recalling that the incident waves a_1 and a_2 must be zero if their respective sources E_1 and E_2 are zero, solving the above equations for the S-parameters gives:

for $E_1 = 1$, $E_2 = 0$, $$S_{11} = 1 - 100I_1 \qquad (43)$$

$$S_{21} = -100I_2 \qquad (44)$$

for $E_1 = 0$, $E_2 = 1$, $$S_{22} = 1 - 100I_2 \qquad (45)$$

$$S_{12} = -100I_1 \qquad (46)$$

Using published values of the model elements as listed in Fig. 10, the scattering parameters over the 2 to 12 GHz range were calculated and plotted as shown in Fig. 19. The element values were then modified to provide a closer fit to scattering parameters of the NEC 244 FET as measured on the network analyzer. These new element values are listed, and the resulting S-parameters are plotted along with the measured S-parameters in Fig. 20.

B. Analysis of Circuit Model

The transmission line model of the FET amplifier circuit shown in Fig. 17 can be analyzed using the theory of two-port networks. The following procedure can be used to calculate the overall scattering parameters of the amplifier:

(1) Calculate the S-parameters of the FET due to shift in reference planes away from the device. The input and output reference planes are shifted through the electrical distances ℓ_3 and ℓ_4, respectively, to obtain matrix $[S']$.

(2) Calculate the transmission parameters of the shifted S-parameter matrix, $[S']$, to obtain matrix $[T']$.

(3) Calculate the transmission parameters of the low impedance transmission line sections ℓ_1 and ℓ_2 to obtain matrices $[T_1]$ and $[T_2]$.

(4) Multiply: $[T_1][T'][T_2] = [T]$, the transmission matrix of the overall amplifier circuit.

(5) Calculate the overall scattering parameters from the matrix $[T]$.

A program was written in BASIC to perform these calculations, given the device S-parameters, frequency, lengths ℓ_1 to ℓ_4, Z_{m1} and Z_{m2}.

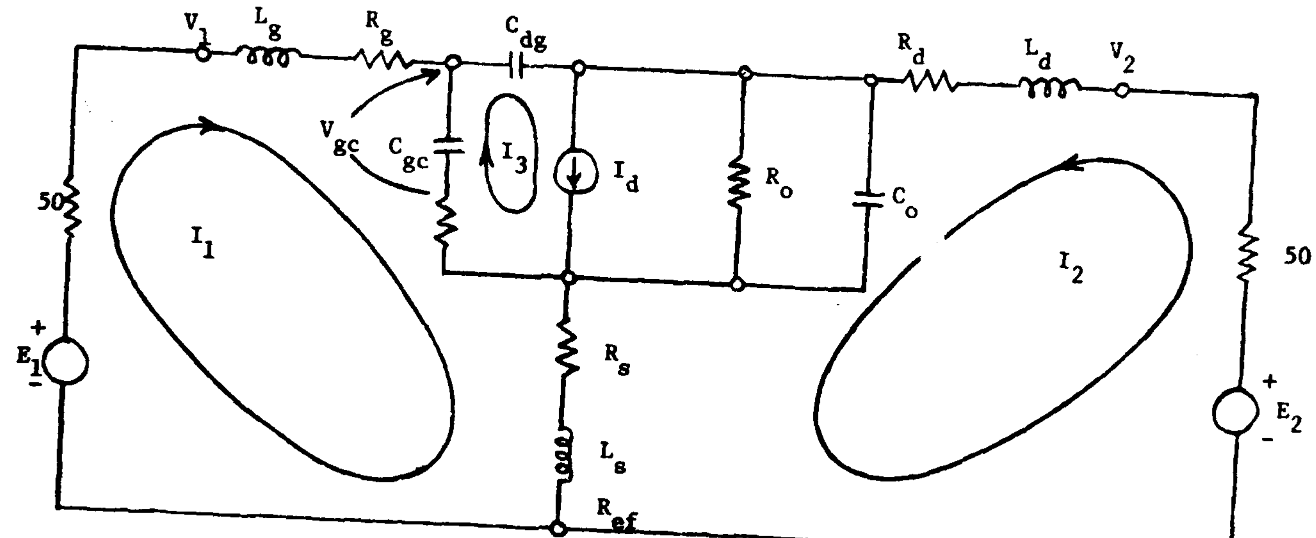

$$I_d = [g_{mo}/(1 + j\omega\tau)]\ V_{gc}$$

Fig. 18. Equivalent Circuit Used to Calculate MESFET Scattering Parameters

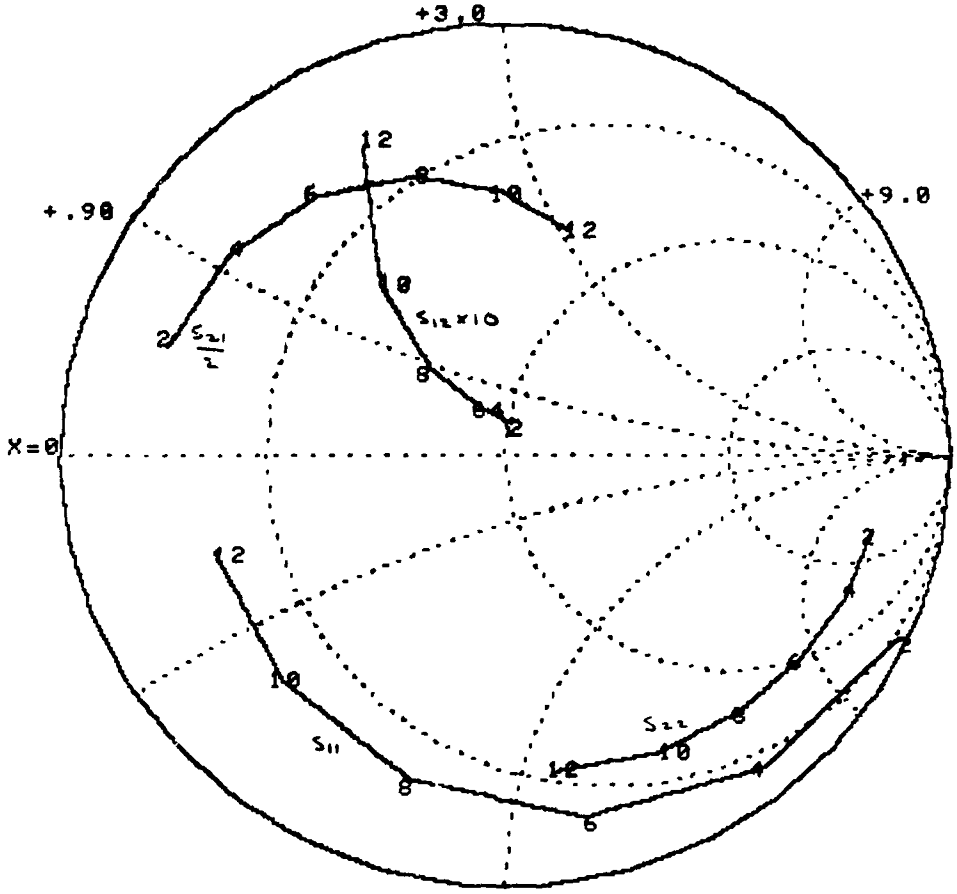

Fig. 19. S-Parameters of NEC 244 FET Calculated from Published Data

```
Program to calculate the S-parameters
of a microwave GaAs FET given the lumped
equivalent circuit element values.
The equivalent circuit is based on a theoretical
device model given by Pucel (IEEE Trans ED).
The element values are entered into data
lines 10 thru 24 as follows:
Ls,Lg,Ld,Rg,Rd,Rc,Ro,f,τ,Cdg,Cgc,Co,gmo
10  DATA 8E-11
11  DATA 2E-10
12  DATA 3E-10
13  DATA 8
14  DATA 2.9
15  DATA .9
16  DATA 300
17  DATA 1.33
18  DATA 1E+10
19  DATA 4.2E-12
20  DATA 5E-15
21  DATA 3.5E-13
22  DATA 1E-13
24  DATA .03
```

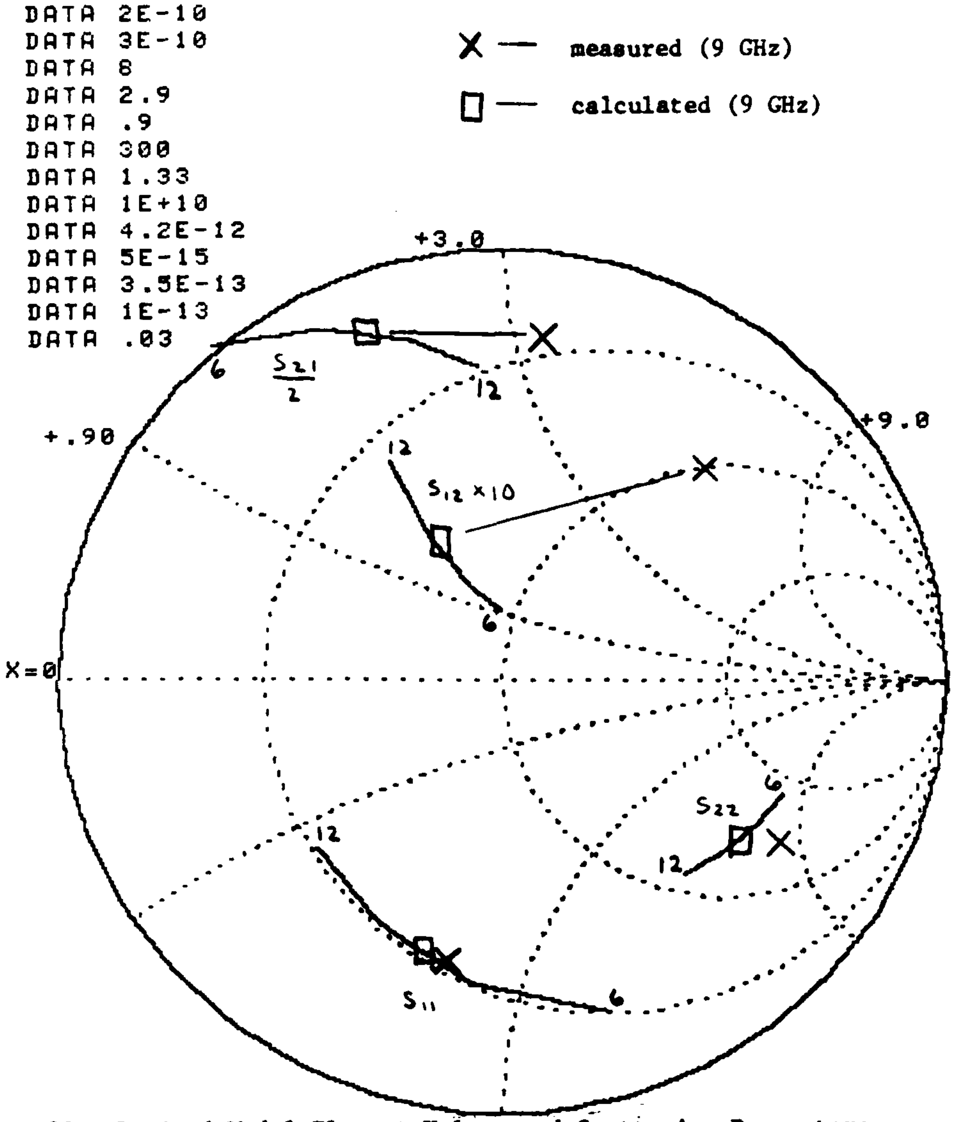

Fig. 20. Revised Model Element Values and Scattering Parameters

The program was used to calculate the overall scattering parameters of the circuit model of Fig. 17 using both measured device S-parameters, and those predicted by the modified equivalent circuit model. The results of the modeling are plotted in Figs. 21 thru 24, along with the measured amplifier performance for comparison.

IV. CONCLUSIONS

An adjustable microstrip matching technique has been developed using metallized ceramic squares (METCHIPs). This structure has demonstrated reproducible performance due to the high degree of flatness of the ceramic material, and due to the uniformity in size afforded by the laser cutting tool. A good impedance transformation over a moderate bandwidth has been demonstrated using METCHIP matching of a low noise GaAs FET amplifier stage at X-band. An empirical model was developed for the METCHIP structure by modifying the transmission line model to account for fringing effects. This modified model was used to construct an overall circuit model for a GaAs FET amplifier stage. An analysis of the overall circuit model showed a close correspondence with the actual measured amplifier characteristics.

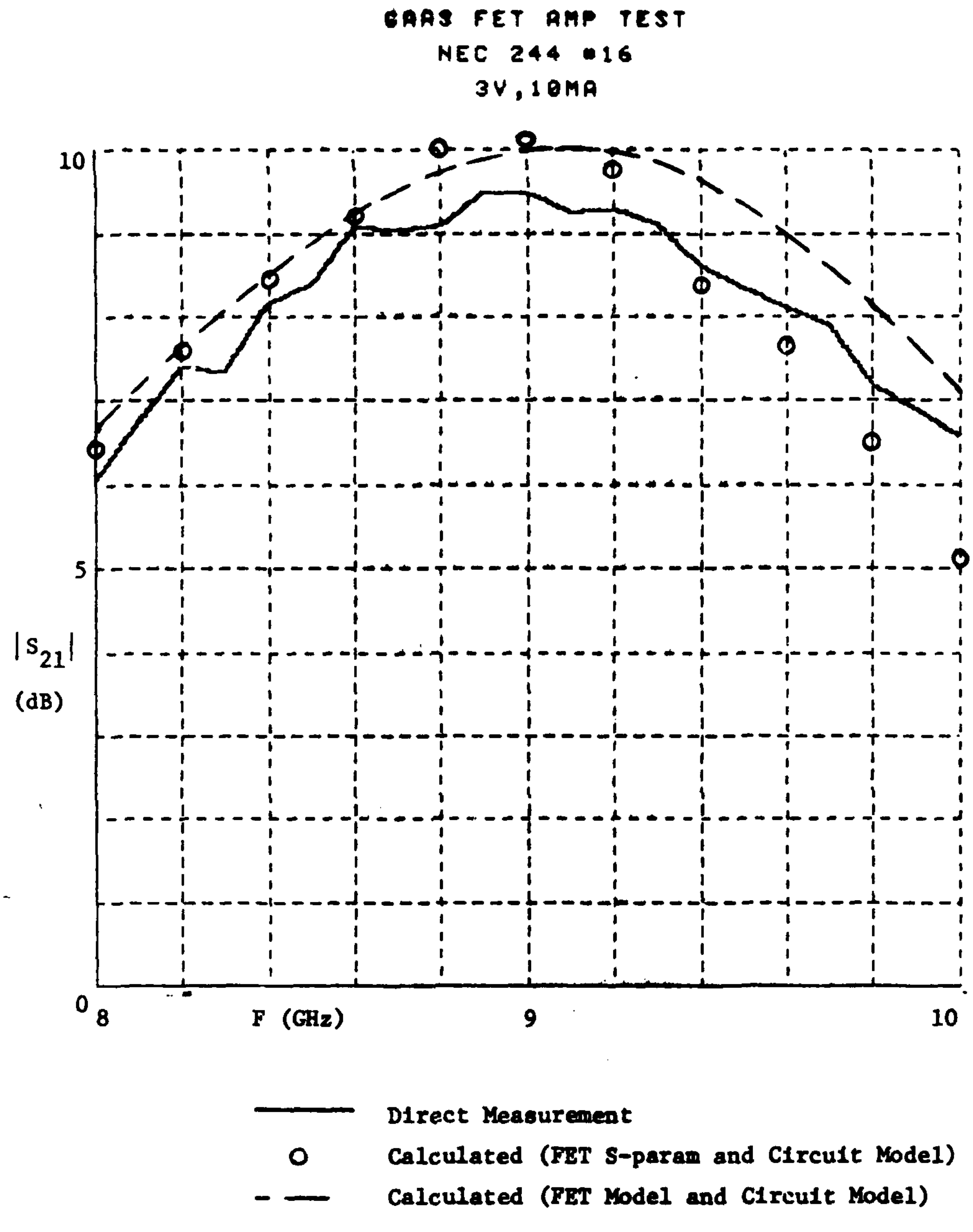

Fig. 21. FET Amplifier Gain

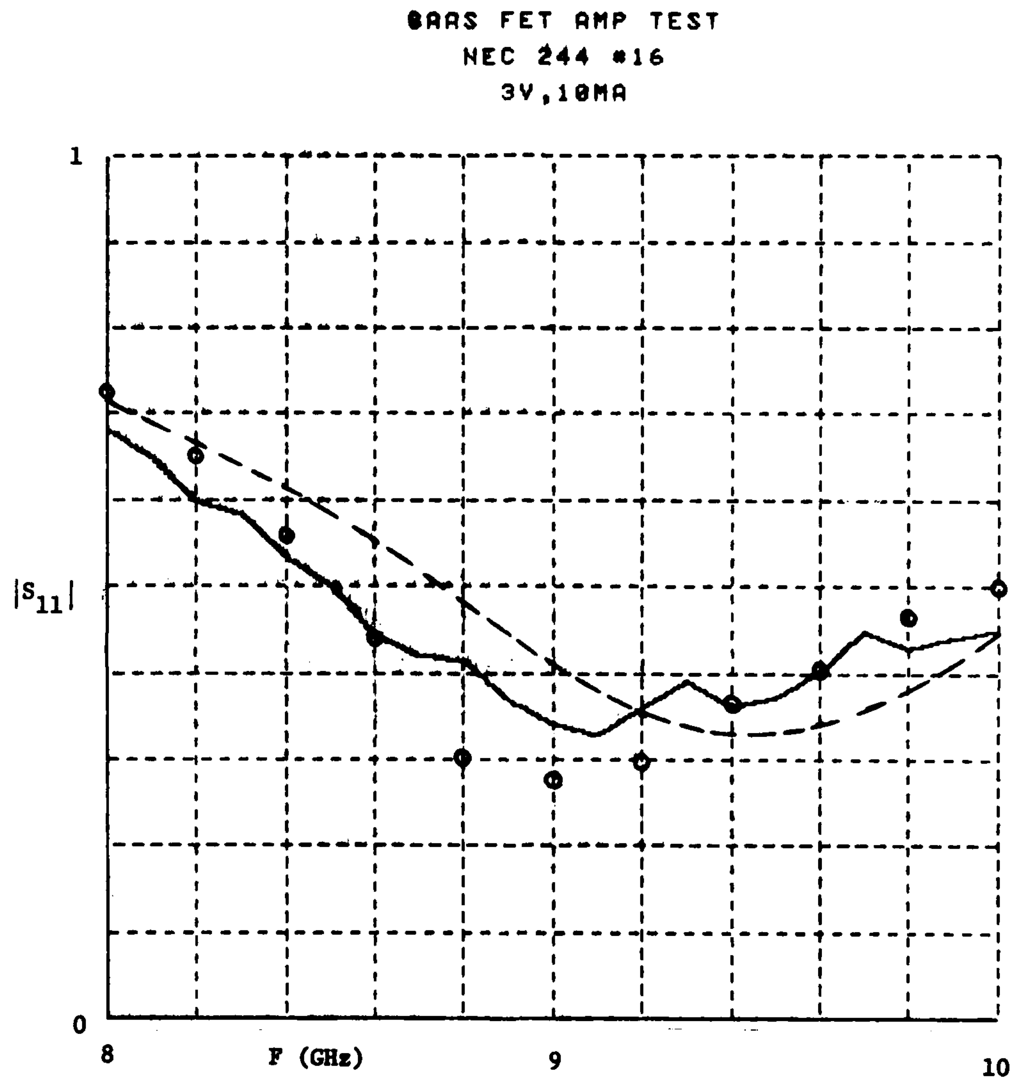

Fig. 22. FET Amplifier Input Reflection Coefficient

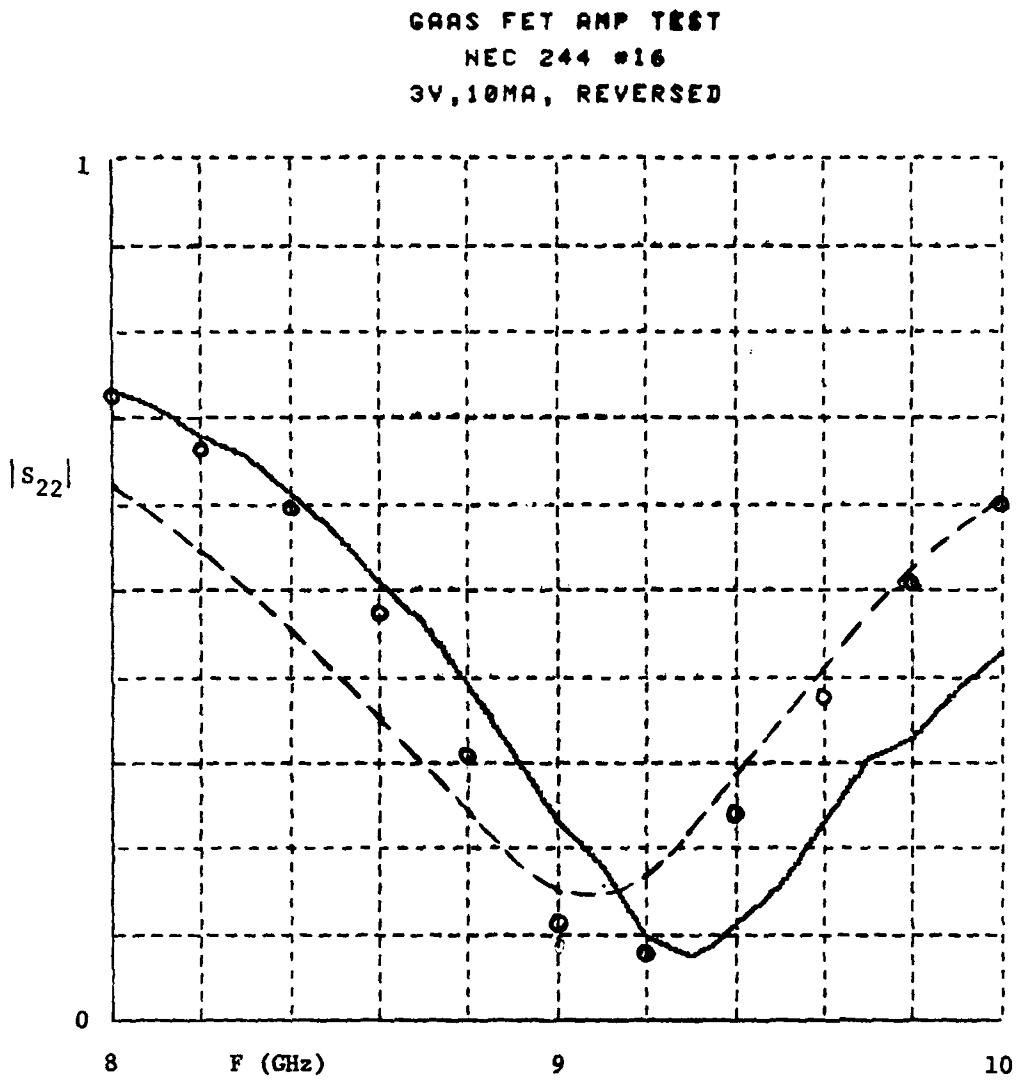

Fig. 23. FET Amplifier Output Reflection Coefficient

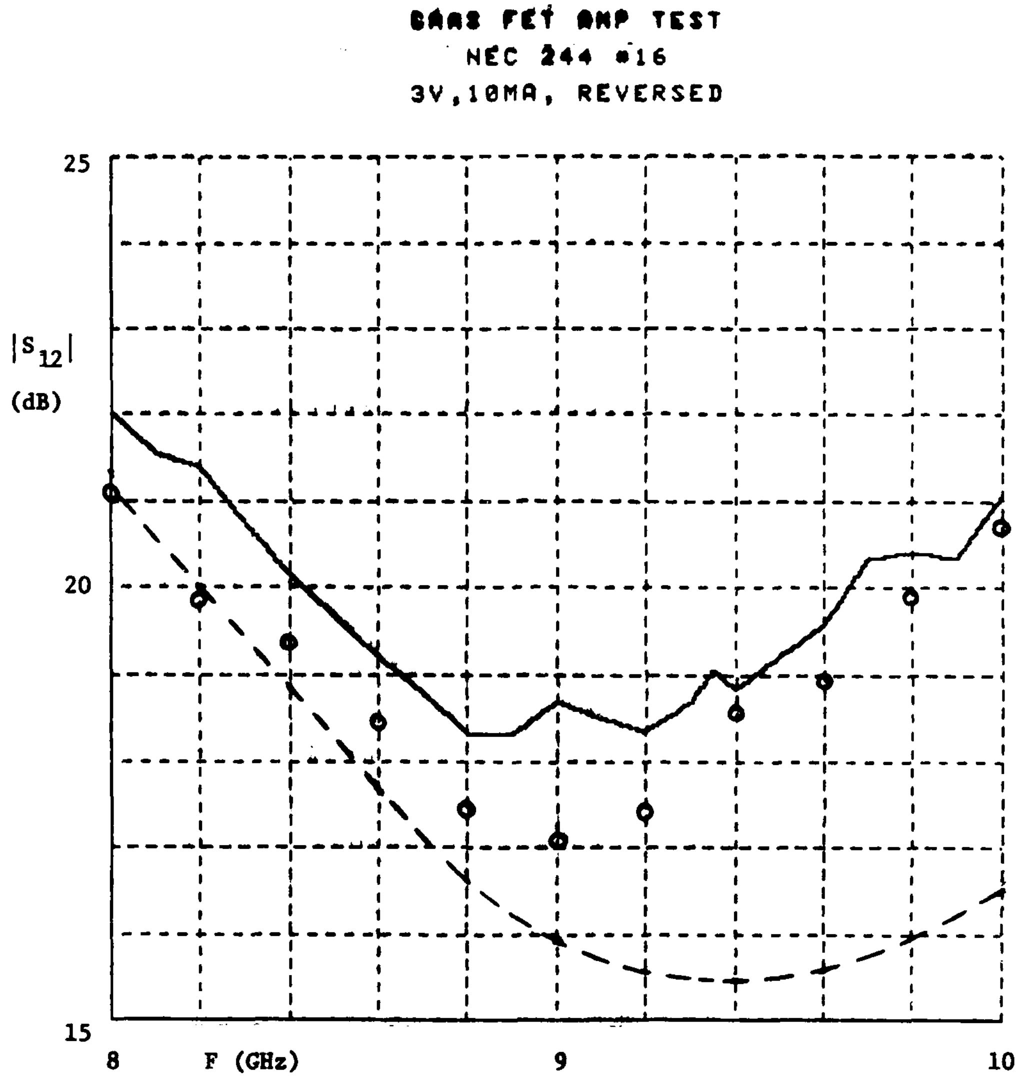

Fig. 24. FET Amplifier Reverse Loss

References

1. H. Sobol, "Extending IC Technology to Microwave Equipment," Electronics, March 10, 1967.

2. Farrar, A., and A. T. Adams, "Matrix Methods for Microstrip Three-Dimensional Problems," IEEE Trans. MTT, Aug. 1972, pp. 497-503.

3. R. L. Sleven, "A Guide to Accurate Noise Measurement," Airborne Instruments Laboratory Application Note, 1966.

4. C. F. Krumm, "Low Noise Field Effect Transistors," Interim Technical Report #2, AFAL Contract F33615-76-C-1114, March 1977.

5. Haus, H. A., and Adler, R. B., "Optimum Noise Performance of Linear Amplifiers," Aug. 1958, Proc. IRE.

6. C. G. Montgomery, "Principles of Microwave Circuits," Dover Publications, Inc., New York, NY, 1965.

7. "A 6 GHz Amplifier Using the HFET-1101 GaAs FET," Hewlett-Packard Application Note 970, February, 1978.

8. W. Baechtold, "Noise Behavior of GaAs Field-Effect Transistors with Short Gate Lengths," IEEE Transcations on Electron Devices, Vol. ED-19, No. 5, May 1972.

9. H. Statz, H. A. Haus, R. A. Pucell, "Noise Characteristics of Gallium Arsenide Field-Effect Transistors," IEEE, TED, Vol. ED-21, No. 9, September 1974.

10. A. van der Ziel, "Solid State Physical Electronics," Prentiss Hall, Inc., Englewood Cliffs, NJ, 1968.

11. "Transistor Parameter Measurements," Hewlett-Packard Application Note 77-1, February, 1967.

12. R. L. Sleven, "A Guide to Accurate Noise Measurement," Airborne Instruments Laboratory Application Note, 1966.

13. "Noise Figure Primer," Hewlett-Packard Application Note 57, January, 1965.

14. J. Frey, T. J. Maloney, "Noise Limits of GaAs and InP Microwave FETs Determined by Dynamic Analysis," Final Report, Contract AFOSR-74-2717.

15. J. F. Cooper and M. S. Gupta, "Microwave Characterization of the GaAs MESFET and the Verification of Device Model," IEEE Journal of Solid State Circuits, June, 1977.

16. G. E. Brehm, G. D. Vendelin, "Biasing FETs for Optimum Performance," Microwaves, February, 1974.

17. W. H. Ku and W. C. Peterson, "Optimum Gain-Bandwidth Limitations of Transistor Amplifiers as Reactively Constrained Active Two-Port Networks," IEEE, TCS, June, 1975.

18. C. A. Mead, "Schottky Barrier Gate Field Effect Transistor," Proc. IEEE, Vol. 54, pp. 307-308, February, 1966.

ATE

LMED

-8